Technical Report

TR-98-22

Development f a kinetic model for the dissolution of the UO2 spent neclear fuel

Application of the model to the minor radionuclides

Jordi Bruno, Esther Cera, Lara Duro, Jordi Pon
QuantiSci SL, Barcelona, Spain

Joan de Pablo
Department Enginyeria Quimica
UPC, Barcelona, Spain

Trygve Eriksen
Department Nuclear Chemistry
KTH, Stockholm, Sweden

May 1998

Svensk Kärnbränslehantering AB
Swedish Nuclear Fuel
and Waste Management Co
Box 5864
SE-102 40 Stockholm Sweden
Tel 08-459 84 00
+46 8 459 84 00
Fax 08-661 57 19
+46 8 661 57 19

Development of a kinetic model for the dissolution of the UO_2 spent nuclear fuel

Application of the model to the minor radionuclides

Jordi Bruno, Esther Cera, Lara Duro, Jordi Pon
QuantiSci SL, Barcelona, Spain

Joan de Pablo
Department Enginyeria Quimica
UPC, Barcelona, Spain

Trygve Eriksen
Department Nuclear Chemistry
KTH, Stockholm, Sweden

May 1998

ABSTRACT

A kinetic model has been developed in order to explain the evolution of the spent fuel matrix/groundwater system. Mass balance equations have been used to follow the evolution of the system with time.

The model has been calibrated by using experimental dissolution data from spent fuel leaching tests from Studsvik (Forsyth et al., 1986) and KTH (Eriksen et al., 1995) and from synthetic unirradiated UO_2 dissolution tests from VTT (Ollila, 1995). The results of the testing exercise indicate that the combination of mass balance equations together with the kinetic rate laws constitute a useful tool to model and explain experimental dissolution data available in the literature for UO_2 solid phases, including uraninites, unirradiated UO_2 and spent fuel. Although the key processes are well identified and understood, there are still some remaining uncertainties concerning some of the critical parameters of the model. This is particularly true for the density of UO_2 sites prone to oxidation and the rates and mechanisms of the hydrogen peroxide and the combined oxygen and bicarbonate promoted dissolution of UO_2 for oxidant concentration ranges relevant to the spent fuel disposal system.

The mass balance kinetic model developed has been extended to minor radionuclides contained in the matrix, i.e. Pu, Tc and Sr. In the case of Pu, the model presented reproduces the behaviour of this critical radionuclide even at early contact times. As it would be expected, Tc seems to follow a different mechanism for its release with respect to the UO_2 matrix dissolution, which is probably linked to the rate of oxidation of Tc metallic inclusions in the fuel. A co-dissolution process of Sr with the UO_2 matrix reproduces the long term dissolution behaviour of this radionuclide, better than the initial Sr release rates.

SAMMANFATTNING

En kinetiskmodell har utvecklats för att förklara utvecklingen av systemet använt bränslematris/grundvatten. Ekvationer för massbalans har använts för att följa systemets utvecklingen med tiden.

Modellen har kalibrerats genom att använda experimentella data för upplösning från lakförsök med använt bränsle från Studsvik (Forsyth et al., 1968) och KTH (Eriksen et al., 1995) och från upplösningsförsök med syntetisk obestrålad UO_2 från VTT (Ollila, 1995). Resultaten från provövningen visar att kombinationen av massbalansekvationer tillsammans med de kinetiska hastighetslagarna utgör ett användbart verktyg för att förklara i litteraturen tillgängliga experimentella upplösningsdata för fasta UO_2 faser, inklusive uraninit, obestrålad UO_2 och använt bränsle. Fastän nyckelprocesserna är väl identifierade och förstådda finns det fortfarande återstående osäkerheter beträffande några av de kritiska parametrarna i modellen. Detta är särskilt sant för tätheten av UO_2 platser benägna för oxidation och hastigheterna och mekanismerna för upplösning av UO_2 befrämjad av väteperoxiden och kombinationen syre och bikarbonat för haltområden relevanta för systemet deponering av använt bränsle.

Den utvecklade massbalanskinetikmodellen har utvidgats till radionuklider som finns i mindre mängd i matrisen, t. ex. Pu, Tc och Sr. För Pu återger modellen denna kritiska radionuklids beteende även för korta kontakttider. Som skulle förväntas tycks Tc följa en annorlunda mekanism för sin frigörelse med avseende på upplösningen av UO_2-matrisen, som troligen är kopplat till oxidationshastigheten för metalliska Tc inneslutningar i bränslet. En samupplösningsprocess av Sr med UO_2-matrisen återger denna radionuklids upplösningsbeteende i det längre tidsperspktivet bättre än initiala frigörelsehastigheterna.

TABLE OF CONTENTS

1. BACKGROUND AND OBJECTIVES

The Swedish Fuel and Nuclear Waste Management Co., SKB is preparing a performance assessment exercise of its high level nuclear waste management concept, under the generic name of SR 97. This assessment requires the application of spent fuel stability models which will incorporate the recent experimental and modelling developments. One particular area where substantial progress has been achieved is in the understanding of the oxidative effects in the spent fuel matrix due to alpha radiolysis. This has been the result of dedicated experimental efforts aimed to understand the mass balance relationships between the oxidants and reductants being produced at the spent fuel-water interface (Eriksen et al., 1995). Furthermore, the development of kinetic mass balance models to explain the observations from these experiments has increased our confidence on the possibility to model and predict the evolution of oxidants with time, as well as their impact on the stability of the UO_2 matrix and the subsequent radionuclide release (Bruno et al., 1996, 1997a). The main building stones of the model are as follows:

* Well controlled experiments on the generation and fate of oxidants produced at the spent fuel/water interface indicate that there is a deficit of oxidants released with respect to the H_2 produced. This deficit has been explained by considering the oxidant uptake by the UO_2 surface (Eriksen et al., 1995).

* There is a well established threshold for the stability of the UO_2 spent fuel matrix, which indicates that the UO_2 cubic structure is able to incorporate additional oxygen without being destabilised up to an oxidative threshold given by the $UO_{2.33}$ phase which corresponds to the nominal U_3O_7 stoichiometry (Allen and Tyler, 1986, Shoesmith and Sunder, 1992). Furthermore, there is mounting evidence that the oxidative alteration of the spent fuel matrix proceeds further via the formation of $UO_3 . xH_2O$, and the subsequent alteration to alkaline earth-uranium (VI) oxyhydroxides (becquerelite) and silicates (soddyite/uranophane), (Forsyth and Werme, 1992, Wronkiewicz et al., 1992, Finch and Ewing, 1991).

* The rate of dissolution of the UO_2 matrix is accelerated by the presence of oxidants and complexing ligands, particularly bicarbonate. (Forsyth and Werme, 1992, Torrero, 1995,)

* The UO_2 spent fuel/water interface is a dynamic redox system and its long-term behaviour can be better approached by using kinetic mass balance models which incorporate the recent developments on surface chemistry, heterogeneous redox processes and the kinetics and thermodynamics of solid/water interaction reactions.

During the last two-three years, a spent fuel oxidation/dissolution model has been developed to be used in the performance assessment of the spent fuel disposal

concept in Sweden. This model has been based on the combination of both kinetic mass balance equations to take into consideration the dynamic redox nature of the spent fuel system and the thermodynamic framework required to explain the long-term evolution of the system.

The kinetic model has been updated and improved by different steps. This report is a compilation of the work performed during this period on the development of this spent fuel kinetic model and its calibration. The main objectives so far achieved have been:

⇒ To develop a kinetic model to explain the evolution of the spent fuel matrix/groundwater system. This model has been based on early contact time data from spent fuel leaching tests from Studsvik (Forsyth et al., 1986) and KTH (Eriksen et al., 1995) and from synthetic UO_2 dissolution tests from VTT (Ollila, 1995).

⇒ To develop a model for the behaviour of plutonium in the spent fuel/groundwater system. Plutonium has been studied separately since it is considered one of the critical radionuclides released by the spent fuel matrix when assessing the safety of the spent fuel disposal system. The model has been based on early contact time data from Studsvik leaching tests (Forsyth and Werme, 1992).

⇒ To test the kinetic model against available dissolution data from spent fuel leaching experiments performed at Studsvik, Tc and Sr dissolution data have been used for this exercise (Forsyth and Werme, 1992 and Forsyth and Eklund, 1995).

2. DEVELOPMENT OF A KINETIC MODEL FOR THE DISSOLUTION OF SPENT FUEL

As we have stated in the Introduction, the purpose of this work has been to develop a kinetic model in order to explain the dissolution of the spent fuel. In this context, mass balance equations have been used to follow the evolution of the system with time.

When studying the stability of the spent fuel we must consider which are the critical master variables that may cause the disruption of the system, i.e., that may induce the release of uranium and of other radionuclides from the spent fuel matrix in contact with groundwater. In principle, the pe, pH and carbonate content constitute the master variables of this chemical system from the thermodynamic stand point. Among these, the pe is the most critical one as visualised in Figure 2.1

In Figure 2-1, the stability fields of UO_2 and of other relevant uranium solid phases are shown as a function of master parameters such as pH and the redox potential (Eh).

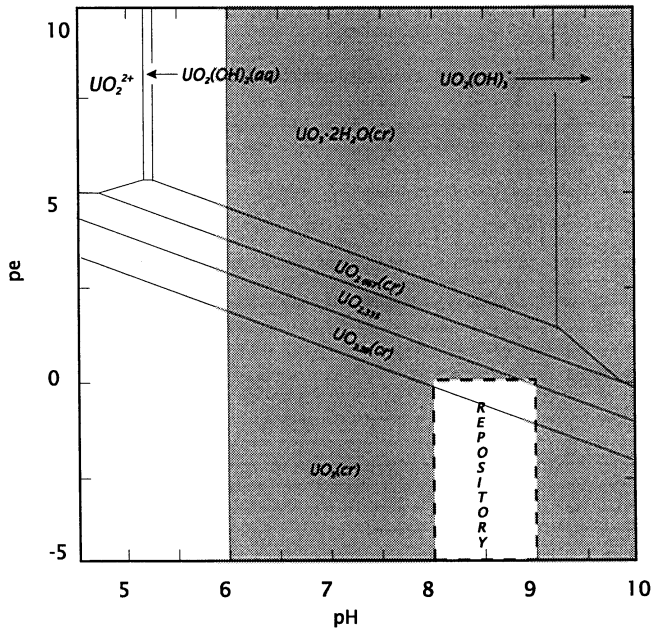

Figure 2-1. *Stability fields of different uranium solid phases (from Grenthe et al., 1992).Shaded area indicates the range of pe and pH values more common in natural groundwaters. The dashed line encloses the pe and pH range more likely to occur under repository conditions.*

We can observe from this figure that the redox potential is the variable which mostly affects the stability of UO_2(fuel) in the pH range of groundwaters (6 to 10). Therefore, oxidant species generated by water-radiolysis represent an important disturbance factor for the stability of the spent fuel/water interface system.

Consequently, the first step in the development of the model has been to perform a careful review of selected experimental data in order to test the combined effect of oxidation and dissolution of the spent fuel matrix.

2.1 EXPERIMENTAL OBSERVATIONS CONCERNING THE OXIDATIVE DISSOLUTION OF THE UO_2 SPENT FUEL MATRIX

A large number of experimental studies have been conducted with the aim of testing the stability of spent fuel under repository conditions. These studies have been carried out either by using spent fuel samples or appropriate analogues of the matrix, such as sintered UO_2 pellets or, to a lesser extent Simfuel.

The dissolution studies cover a wide range of experimental conditions regarding the redox state of the system and the composition of the water used (deionised water, granitic groundwater, etc.). This should in principle allow a better understanding of the behaviour of the system under different physico-chemical conditions.

The data selected to test the kinetic model are those obtained under conditions which are similar to those expected in a repository. This is oxic conditions and bicarbonate solutions, in order to test the combined effect of oxidant generation due to α-radiolysis and the presence of carbonate ligands on the dissolution of the spent fuel matrix. However, as we will discuss later on, the oxidising effect in aerated solutions overtakes the potential radiolytic generation of oxidants under anoxic conditions.

2.1.1 Solution chemical studies

In general most of the kinetic studies indicate an initially fast uranium release at the early contact times, followed by a somewhat slower dissolution rate at longer times.

Table 2-1 is a summary of the experimental observations. One interesting observation is that the determined dissolution rates for the various types of samples (pure UO_2, spent fuel and Simfuel) fall in the same range both in the initial dissolution step and the final evolution steps. This is a clear indication that the same mechanism operates for both irradiated and non-irradiated samples under aerated oxic conditions and in bicarbonate solutions.

The initial dissolution rate (R_1) is larger than the dissolution rate of the second period (R_2), independently of the type of sample studied and of the experimental conditions. The difference between R_1 and R_2 values is approximately of one order of magnitude.

Dissolution rates have been calculated as an average of the different values determined from experimental results. As it can be seen in Table 2-1, the standard deviation of the dissolution rates determined from experiments performed with

Simfuel samples is larger than the measure itself. This large dispersion does not give confidence in the determined values. Therefore, we have not considered these results in the model.

In the experiments with low Surface Area/Volume ratio, no secondary phase formation was observed (Bruno et al., 1995; Casas et al., 1994; Ollila, 1995). On the other hand, in the experiments where this ratio was higher, the precipitation of secondary phases, such as schoepite, was observed after the dissolution process (Ollila, 1995; Wronkiewicz et al., 1992). In spent fuel dissolution experiments in deionised water, i.e. in the absence of complexing ligands the precipitation of dehydrated schoepite has also been observed (Forsyth and Werme, 1992).

Uranium released from a UO_{2+x} sample under anoxic conditions (Bruno et al., 1991), indicated a dissolution rate of $2.76 \cdot 10^{-12}$ mole·dm^{-2}·s^{-1}, considering $[HCO_3^-]=10^{-3}$ mole·dm^{-3} and pH=8. This value is similar to the dissolution rates shown in Table 2-1. This indicates that the first dissolution period in all these experiments was dominated by the dissolution of the initially oxidised surface layer observed in the XPS analyses, independently of the redox conditions.

Based on the experimental observations, the overall rate of matrix dissolution has been separated into two differentiated terms:

$$R_{ov} \begin{cases} R_1 \text{ for } t<t_1 \\ R_2 \text{ for } t>t_1 \end{cases} \qquad 2\text{-}1$$

where:

R_1 is the rate of dissolution of the initial oxidised layer (UO_{2+x})

R_2 is the final rate of dissolution of the matrix, which will depend on different processes, basically the oxidation of the co-ordination sites and their dissolution.

t_1 is the time at which the initial oxidised layer has been dissolved.

This initial R_1 process is important to analyse the experimental observations but is of little relevance for the long term behaviour of the disposal system.

Table 2-1. Experimental observations: Oxic conditions, $[HCO_3^-]=10^{-2}$-10^{-3} M, pH ≅ 8, at room temperature.

	UO_2		SIMFUEL		SPENT FUEL	
	Batch	**Flow**	**Batch**	**Flow**	**Batch**	**Flow**
R_1(mole×dm^{-2}×s^{-1})	$1.37 \cdot 10^{-12}$ $\pm 6.45 \cdot 10^{-13}$ (Bruno et al., 1995) from data in (Ollila, 1995)		$6.95 \cdot 10^{-13}$ (Bruno et al., 1995)		$1.13 \cdot 10^{-13}$ from data in (Forsyth et al., 1986)	
R_2(mole×dm^{-2}×s^{-1})	$4.72 \cdot 10^{-13}$ $\pm 2.06 \cdot 10^{-13}$ (Bruno et al., 1995)	$1.56 \cdot 10^{-12}$ $\pm 6.36 \cdot 10^{-14}$ (Bruno et al., 1995)	$2.09 \cdot 10^{-14}$ $\pm 5.08 \cdot 10^{-14}$ (Bruno et al., 1995) (Casas et al., 1991)	$2.94 \cdot 10^{-14}$ $\pm 5.51 \cdot 10^{-14}$ (Bruno et al., 1995) (Casas et al., 1991)	$1.18 \cdot 10^{-14}$ (Forsyth et al., 1986)	$1.68 \cdot 10^{-12}$ $\pm 1.24 \cdot 10^{-13}$ (Gray et al., 1992)
S/V (m^{-1})	12, 226 and 590		15		No information available*.	
Secondary phases	No precipitation of secondary phases observed. (Bruno et al., 1995) (Ollila, 1995) 37000, 622000 Precipitation of secondary phase in the experiment with the highest S/V ratio. (Ollila, 1995) (Wronkiewicz et al., 1992)		No information available.		In the absence of carbonate in solution and in batch experiments, $UO_3 \cdot 0.8H_2O$ have been identified (Forsyth and Werme, 1992)	

Anoxic conditions: $R_1 = 2.76 \cdot 10^{-12}$ mole·dm^{-2}·s^{-1} (Bruno et al.,1991)

*. Rates calculated by using BET data provided by SKB (Lars Werme, pers. comm.): 30-250 cm^2/g.

2.1.2 Surface spectroscopic information

Surface spectroscopy (XPS) of the reacting solids show the following general trends:

* Initially, the solid surface is fairly oxidised, with a relatively large U(VI) content. The surface composition corresponds to an stoichiometry close to $UO_{2.67}$ (Casas et al., 1994).

* The reacted surface has a lower U(VI)/U(IV) ratio, corresponding to stoichiometries close to $UO_{2.33}$ in the experiments performed at neutral and alkaline pH values (Casas et al., 1994).

* XPS analyses in combination with electrochemical experiments performed with nuclear fuel, UO_{2+x}, within the Canadian programme (Shoesmith and Sunder, 1991, Sunder et al., 1992), have shown that significant oxidative dissolution starts once the surface composition approaches $UO_{2.33}$ stoichiometry. Oxidation at potentials beyond this threshold leads to dissolution as uranyl ions.

Precipitation of secondary phases has been observed in some dissolution experiments (Forsyth and Werme, 1992 in deionised water, Shoesmith et al., 1989 in $NaClO_4$ 0.1 mole·dm^{-3}, Wronkiewicz et al., 1992 in J13 water, Ollila, 1995 in synthetic granitic groundwater).

2.2 PROCESSES AFFECTING THE DISSOLUTION BEHAVIOUR OF THE SPENT FUEL MATRIX IN CONTACT WITH GROUNDWATER AND PARAMETERS REQUIRED BY THE MODEL

In this section we will discuss which are the main processes involved in the oxidative dissolution of the spent fuel matrix as well as the key parameters required to model its long term behaviour.

2.2.1 Processes

By taking into account the experimental observations, we have considered that the main processes occurring in the system are:

Process 1. R*adiolytic generation of oxidants*, expressed by the following reaction:

$$H_2O + \alpha\text{-radiolysis} \Rightarrow \text{oxidants} \qquad 2\text{-}2$$

where oxidants stands for the main oxidants generated in the system, namely O_2, and H_2O_2. This generation occurs at a rate R_{rad}.

Process 2. O*xidation of the surface* of spent fuel:

$$\left(> UO_2\right)_n \equiv UO_2 + 0.334\,H_2O \Rightarrow$$
$$\Rightarrow \left(> UO_2\right)_n \equiv U^{IV}_{0.667}U^{VI}_{0.334}O_{2.334} + 0.667\,H^+ + 0.667\,e^- \qquad 2\text{-}3$$

where $(>UO_2)_n \equiv UO_2$ stands for the unoxidised surface layer, while $(>UO_2)_n \equiv U^{IV}_{0.667}U^{VI}_{0.334}O_{2.334}$ stands for the resulting oxidation of a surface monolayer.

Process 3. *Reduction of the oxidants* present in the system. The main oxidant species produced by radiolysis of water are O_2 and H_2O_2, whose reduction reactions can be expressed as follows:

$$O_2 + 4H^+ + 4e^- \Leftrightarrow 2H_2O \qquad 2\text{-}4$$

$$H_2O_2 + 2H^+ + 2e^- \Leftrightarrow 2H_2O \qquad 2\text{-}5$$

The combination of Process 2 and Process 3 gives us the overall process of oxidation of spent fuel by O_2,

$$\left(> UO_2\right)_n \equiv UO_2 + 0.167O_2 \Rightarrow \left(> UO_2\right)_n \equiv U^{IV}_{0.667}U^{VI}_{0.334}O_{2.334} \qquad 2\text{-}6$$

and by H_2O_2,

$$\left(> UO_2\right)_n \equiv UO_2 + 0.334H_2O_2 \Rightarrow \left(> UO_2\right)_n \equiv U^{IV}_{0.667}U^{VI}_{0.334}O_{2.334} + 0.334H_2O \qquad 2\text{-}7$$

occurring at a rate R_{ox}.

Process 4. D*issolution of the oxidised spent fuel*, i.e., the release of uranium to the solution, described by the following expression:

$$\left(> UO_2\right)_n \equiv U^{IV}_{0.667}U^{VI}_{0.334}O_{2.334} + 0.667H^+ \Rightarrow$$
$$\Rightarrow \left(> UO_2\right)_n \equiv \left(UO_2\right)_{0.667} + 0.334UO_2^{2+} + 0.334H_2O \qquad 2\text{-}8$$

occurring at a rate R_{diss}.

The U(VI) aqueous speciation will depend on the aqueous chemistry of the system. Thus, in principle two different processes can be proposed at pH in the range 7 to 8 for the dissolution of the oxidised uranium depending on the absence or the presence of carbonate in the system (Figure 2-2).

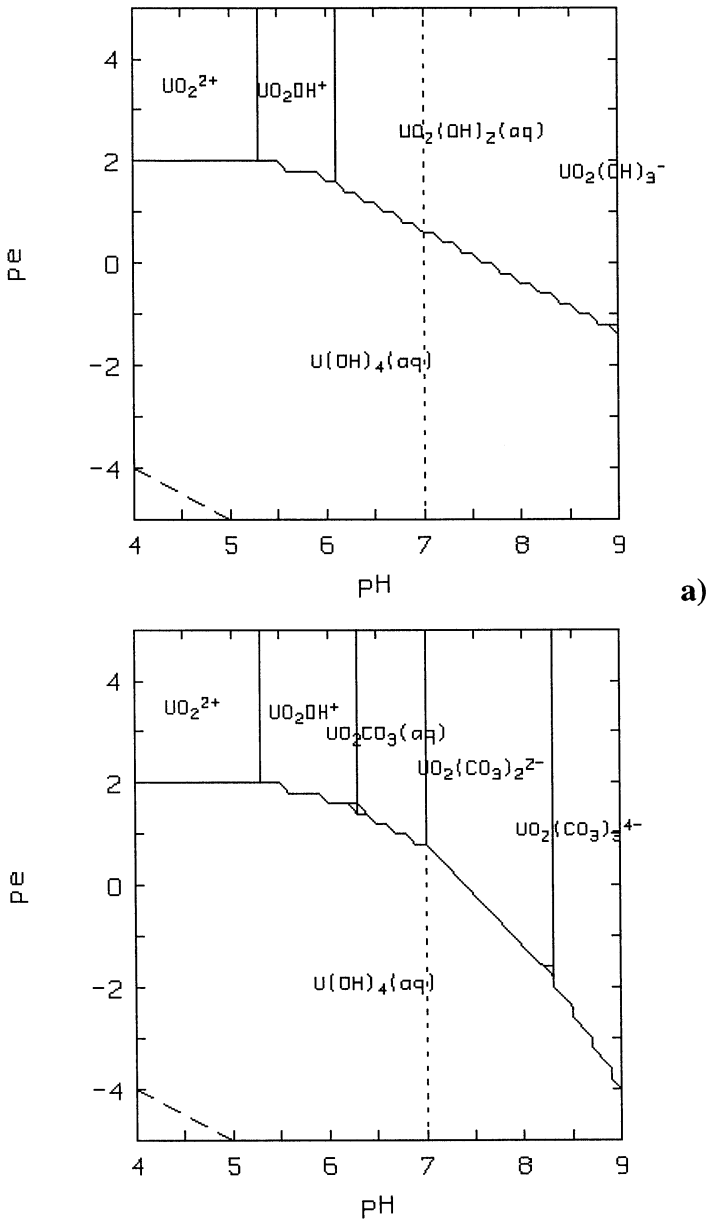

Figure 2-2. *Predominance diagrams of aqueous uranium complexes.* ***a)*** *in the absence of carbonate,* ***b)*** *in the presence of carbonate ($[CO_3^{2-}]_{tot}=10^{-3}$ mole·dm^{-3}) in the system. $[U]_{tot}=5\cdot10^{-7}$ mole·dm^{-3}. Thermodynamic database used SKBU (Bruno and Puigdomènech, 1989).*

Therefore, in the absence of carbonate in the system, $UO_2(OH)_2(aq)$ becomes the predominant aqueous species with the following stoichiometry for the dissolution process:

$$\left(> UO_2\right)_n \equiv U^{IV}_{0.667}U^{VI}_{0.334}O_{2.334} + 0.334H_2O \Rightarrow$$
$$\Rightarrow \left(> UO_2\right)_n \equiv \left(UO_2\right)_{0.667} + 0.334UO_2(OH)_2 \qquad 2\text{-}9$$

If carbonate is present in the system, $UO_2(CO_3)_2^{2-}$ becomes the predominant species. The dissolution process is given by the reaction:

$$(> UO_2)_n \equiv U^{IV}_{0.667}U^{VI}_{0.334}O_{2.334} + 0.667HCO_3^- \Rightarrow$$

$$\Rightarrow (> UO_2)_n \equiv (UO_2)_{0.667} + 0.334UO_2(CO_3)_2^{2-} + 0.334H_2O$$

2-10

As we have already pointed out and despite of the fact that several experimental observations on the dissolution of unirradiated UO_2(s) (Ollila, 1995; Casas et al., 1994) indicated an initially oxidised surface layer, this is a very transient phenomenon with little relevance for the long term behaviour. Hence, we have neglected this initial stage in the formulation of the model (Bruno et al., 1996). This is equivalent to eliminate R_1 in equation 2-1.

2.2.2 Estimation of the rate of oxidant generation by α-radiolysis of water. Process 1 (R_{rad})

The production rate of the radiolytically generated oxidants has been calculated by several authors by including the known kinetic on heterogeneous production, consumption and recombination of radiolytic products (Christensen, 1990, Christensen et al., 1994, Eriksen, 1996).

2.2.3 Estimation of the rate of oxidation of the spent fuel matrix and the subsequent dissolution of the oxidised surface layer

One of the assumptions underlying our model is that for uranium to be dissolved, it must be previously oxidised to the U(VI) oxidation state. Therefore, we need to separate the dissolution rate obtained from experimental studies (R_2) into two components:

* a first term representing the oxidation of U(IV) to U(VI), and

* a second term, which stands for the dissolution of U(VI)

This separation is difficult because the experimentally measured variables (mainly the concentration of uranium in solution) allow us only the quantification of the overall dissolution processes. To separate the oxidation and dissolution contributions is complex at this stage.

Rate of oxidation of spent fuel. Processes 2 and 3 (R_{ox})

The processes of oxidation have been expressed by the following equations:

$$(> UO_2)_n \equiv UO_2 + 0.167\ O_2 \Rightarrow (> UO_2)_n \equiv U^{IV}_{0.667}U^{VI}_{0.334}O_{2.334}$$

2-6

$$(> UO_2)_n \equiv UO_2 + 0.334\ H_2O_2 \Rightarrow (> UO_2)_n \equiv U^{IV}_{0.667}U^{VI}_{0.334}O_{2.334} + 0.334H_2O$$

2-7

.

Most of the studies on the dissolution kinetics of unirradiated $UO_2(s)$ and Simfuel available in the literature are performed under aerated oxic conditions, this applies also for spent fuel studies. The main oxidants produced by radiolysis are molecular oxygen and hydrogen peroxide and, therefore, most of the effort has been devoted to ascertain the mechanisms or, at least the empirical expression of the rate, of oxidation/dissolution of spent fuel as a function of the concentration of those two oxidant species, i.e., to find an expression of the type:

$$R_{ox} = k_{H2O2} \times [H_2O_2]^m + k_{ox} \times [O_2(aq)]^n \qquad 2\text{-}11$$

The usual way of extracting the dependence expressed in equation 2-11 is to measure the rate of dissolution of the solid under variable oxidant concentration, while other chemical and physical variables are kept constant.

$UO_2(s)$ and spent fuel oxidation by hydrogen peroxide. Hydrogen peroxide promoted dissolution rates.

The mechanistic information concerning the influence of hydrogen peroxide on UO_2 dissolution is rather limited. This is mainly because of the experimental difficulties associated to the instability of hydrogen peroxide and not to the relevance of the kinetic information (the famous Diogenes lamp effect).

In principle, we are only aware of four studies concerning the effect of hydrogen peroxide on the oxidative dissolution of UO_2, these are the work by Hiskey (1980), Shoesmith and Sunder (1992), Christensen (1991) and Giménez et al. (1996).

⇒ The first set of data used for the selection of the rate of oxidation of spent nuclear fuel by hydrogen peroxide is taken from experiments performed by Shoesmith and Sunder (1992) within the Canadian program. These authors report a variable value of the parameter m in equation 2-11 depending on the concentration of hydrogen peroxide. They distinguish three different regions:

* for $[H_2O_2] > 5 \cdot 10^{-3}$ mole·dm^{-3} the rate law reported is $R_{ox} = k_{H2O2} \times [H_2O_2]$, i.e., linear dependence of the oxidation rate on the concentration of H_2O_2. From the graphical data presented in Shoesmith and Sunder (1992) a value of $k_{H2O2} \approx 1.2 \cdot 10^{-10}$ can be estimated, when R_{ox} is expressed in mole·dm^{-2}·s^{-1}.

* for $2 \cdot 10^{-4} < [H_2O_2] < 5 \cdot 10^{-3}$ mole·dm^{-3}, constant R_{ox} values, independent of the $[H_2O_2]$ are reported. From the graphical data presented, the value R_{ox} (= k_{H2O2}) $\approx 5 \cdot 10^{-13}$ mole·dm^{-2}·s^{-1} can be estimated.

* for $[H_2O_2] < 2 \cdot 10^{-4}$ mole·dm^{-3}, the authors report a rapid decrease in the value of R_{ox} as the oxidative dissolution threshold is approached.

⇒ Christensen (1991) reports results on the dissolution rate of UO_2 at hydrogen peroxide concentrations of $5 \cdot 10^{-2}$ mole·dm^{-3}, at which the measured rate for the dissolution of spent fuel is $2.14 \cdot 10^{-11}$ mole·dm^{-2}·s^{-1}. In this range of

concentration of hydrogen peroxide, the dissolution rate can be expressed as: $R_{ox} = k_{H2O2} \times [H_2O_2]$ -see Shoesmith and Sunder (1991) comments- and, therefore we can calculate a value of $k_{H2O2} = 4.28 \cdot 10^{-10}$ when R_{ox} is expressed in mole·dm^{-2}·s^{-1} , which is three times larger, but still in the order of the one obtained by Shoesmith and Sunder when working in this range of hydrogen peroxide concentrations.

⇒ The experimental observations of Giménez et al. (1996) support these findings, since these authors report a linear dependence (0.99 ± 0.07) of the dissolution rate of unirradiated UO_2(s) on the H_2O_2 concentration for $[H_2O_2] \geq 10^{-2}$ mole·dm^{-3}, with a value of $k_{H2O2} = 8 \cdot 10^{-11}$ when the value of R_{ox} is expressed in mole·dm^{-2}·s^{-1}. No variation in the dissolution/oxidation rate is observed by these authors at $[H_2O_2] = 10^{-3}$ mole·dm^{-3}, and a value of $9 \cdot 10^{-13}$ mole·dm^{-2}·s^{-1} is reported in this case, very similar to the one estimated from the data reported by Shoesmith and Sunder (1992).

⇒ The data obtained by Hiskey (1980) deserves a more careful discussion. The author studied the kinetics of oxidative dissolution of UO_2(s) by H_2O_2 in aqueous $(NH_4)_2CO_3$ media where the total carbonate concentration varied from 0.005 to 0.5 mole·dm^{-3}.

The results obtained at a constant total concentration of carbonate of 0.5 mole·dm^{-3} are shown in Figure 2-3.

Hiskey obtained the following expression for the rate of oxidative dissolution of UO_2(s):

$$R_{ox} = k \times [H_2O_2]^{0.5} \times [HCO_3^-]_{tot}^{0.45} \text{ mole·dm}^{-2}\text{·s}^{-1} \qquad 2\text{-}12$$

with $k = 6.83 \cdot 10^{-7}$

The fractional dependence of the oxidative dissolution rate on the total carbonate concentration is comparable to the one obtained by Torrero (1995), who found a value of 0.42 ± 0.08.

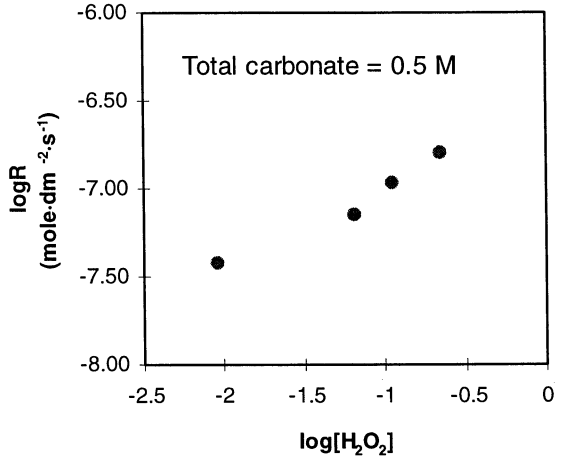

Figure 2-3. *Rate values obtained as a function of the hydrogen peroxide concentration (from Hiskey, 1980).*

The rates obtained by Hiskey are neither comparable to the ones obtained by Giménez et al. (1996) nor to the ones from Shoesmith and Sunder (1992). This is probably because these data was obtained in quite concentrated ammonium carbonate solutions with a much larger alkalinity than the one used in the other two studies. This is bound to have implications on the operating mechanism. The study was performed in order to optimise the oxidative leaching of uranium ores, which is not exactly the objective of our waste management related studies. In addition the publication by Hiskey contains some inconsistencies between the reported data in Tables and Figures, hence we have decided not to give more consideration to these data in the further development of the model.

We consequently selected a rate constant and rate order in accordance with the ones proposed by Shoesmith and Sunder and by Giménez et al. Therefore, the average of the R_{ox} in the presence of H_2O_2 is the one shown below:

$$R_{ox} = (2.1\pm1.5)\cdot10^{-10}\times[H_2O_2] \text{ mole U}\cdot\text{dm}^{-2}\cdot\text{s}^{-1} \text{ for } [H_2O_2]>5\cdot10^{-3} \text{ mole}\cdot\text{dm}^{-3} \quad 2\text{-}13$$

Mechanisms and rates of oxidation of natural uraninites, UO_2(s) and spent fuel by molecular oxygen. Oxygen promoted dissolution rates.

Following the Diogenes lamp saga and because the experimental procedure under a controlled oxygen atmosphere is simpler than the one required to work under constant H_2O_2 solutions, there are far more studies available in the literature on the effect of dissolved oxygen on the rate of oxidation/dissolution of UO_2(s) and/or spent fuel than on the effect of H_2O_2. This is particularly true for experiments performed in solutions in contact with air.

As it is generally the case in mechanistic studies, the reaction order with respect to the main reactant (molecular oxygen in this case) can be quite varying depending on the concentration range used in the experiments. This is something we have already discussed for the hydrogen peroxide promoted dissolution and it is more evident in the oxygen promoted dissolution of UO_2.

Reaction orders for the oxygen promoted dissolution of UO_2 vary between 0 an 1 depending on the experimental conditions, in terms of temperature, oxygen concentration, carbonate concentration or type of solid. What follows is a discussion of the available published data in order to bring some rationale for the selection of potential reaction order rates with respect to oxygen to be applied to the spent fuel disposal conditions.

We have only considered data collected under the conditions that prevented the precipitation of secondary phases. The review is made in chronological order and takes into consideration work performed with all kinds of UO_2 phases: natural uraninites, spent fuel and synthetic uranium dioxide.

⇒ One of the first studies on the kinetics of UO_2 dissolution was performed by Grandstaff (1976) in his seminal Ph.D. work on the influence of various environmental parameters on the kinetics of dissolution of natural uraninites. This work was later used by Holland (1984) as a basis for establishing oxygen levels in the Precambrian atmosphere by studying the alteration of uraninites from the Athabaska basin. The author performed a careful experimental study on the dependence of the dissolution rate of uraninite as a function of the organic matter content, the carbonate concentration, the pH, the temperature, the mole fraction of non uranium cations in the uraninite lattice, and the dissolved oxygen concentration. He worked in pO_2 ranges lower than 0.2 atm (from pO_2 0.002 to 0.02 atm), and at pH between 4 and 7 and he found a nearly linear dependence of the rate of oxidation/dissolution on the dissolved oxygen concentration (**n ≈ 1**).

⇒ The result of a similar work performed by the Princeton school is reported by Posey-Dowty et al. (1987). These authors worked at oxygen partial pressures from 0.2 to 4 atm and at pH between 7.2 and 8 and found a 0.5 rate order of the oxygen promoted dissolution of natural uraninites with respect to the dissolved oxygen concentration (**n = 0.5**).

⇒ Within the Canadian programme, Shoesmith and Sunder (1991) studied the dissolution of CANDU fuel by electrochemical methods on $NaClO_4$ solutions purged with nitrogen gas containing different percentages of oxygen (from 0 to 100%), at pH 9.5 and reported a linear dependence of the oxidation of CANDU fuel on the oxygen concentration (**n = 1**) for $[O_2]aq > 5 \cdot 10^{-6}$ mole·dm^{-3}. At 0.2 atm of oxygen, and at room temperature, values of the rate around 10^{-13} mole of U·dm^{-2}·s^{-1} are obtained by these authors.

⇒ By using also electrochemical methods in dilute alkaline aqueous solutions ($NaClO_4$ 0.1 mole·dm^{-3} at pH = 9.5), Hocking et al. (1992) obtained values of n close to **1** when studying the oxidation of CANDU fuel, and values of n close to **0.5** in the case of a different fuel sample from a different origin (El Dorado Nuclear).

⇒ In a later work, by using also electrochemical methods under different aqueous solutions ($NaClO_4$/$NaHCO_3$/Na_2CO_3) and at several oxygen aqueous concentrations ranging between 10^{-5} to 10^{-3} mole·dm^{-3}, Hocking et al. (1994) report linear dependence of the rate of oxidation of CANDU pellets on the oxygen concentration (**n = 1**) and they observed no influence of the carbonate concentration on the value of n.

⇒ Within the American programme for spent fuel disposal, Gray et al. (1992) have performed a large experimental effort studying the dependence of the spent fuel dissolution rate in several physico-chemical parameters, including: the temperature, the pH and the total carbonate concentration, obtained with an oxygen atmospheric content. The kinetic data was fitted to the following equation:

$$\log R = 7.45 + 0.26 \times \log[CO_3]_{tot} + 0.14 \times \log[H^+] - 1550/T \qquad 2\text{-}14$$

when R is expressed in $mgU \cdot m^{-2} \cdot d^{-1}$, and T in K.

⇒ In a later work, Gray and Wilson (1995) presented their experimental data on the rate of oxidative dissolution measured at different dissolved O_2 concentration and obtained the following values for n depending on the conditions of the experiments ($R_{ox} = k_{ox} \times [O_2]^n$):

* **n = 0.5** for experiments performed with unirradiated UO_2 in $10^{-6} < pO_2 < 0.2$ atm at room temperature at pH between 8 and 10, with $[CO_3]_{tot} = 2 \cdot 10^{-4}$ $mole \cdot dm^{-3}$.

* **n = 0.39** for the same series of experiments but when considering only those results obtained for the upper pO_2 range: $10^{-3} < pO_2 < 0.2$ atm at pH between 8 and 10.

* **n = 0.05** for experiments performed with spent fuel in solutions with a carbonate concentration ranging between $2 \cdot 10^{-4}$ and $2 \cdot 10^{-2}$ $mole \cdot dm^{-3}$, a partial oxygen pressure in the range of $3 \cdot 10^{-3} < pO_2 < 0.2$ atm at 25°C and at pH between 8 and 10.

* **n = 0.79** for experiments performed with spent fuel in solutions with higher carbonate concentration and temperature: $[CO_3]_{tot} = 2 \cdot 10^{-2}$ $mole \cdot dm^{-3}$ and $10^{-3} < pO_2 < 0.2$ atm at 75°C at pH between 8 and 10.

From these results it can be observed that, at room temperature, the increase in the oxygen content causes a decrease in the value of n.

At room temperature the rate values measured vary between 10^{-13} and $2 \cdot 10^{-12}$ mole of $U \cdot dm^{-2} \cdot s^{-1}$. At pH around 8, 0.2 atm of O_2 and 1mM total carbonate in solution, a value of $1.2 \cdot 10^{-12}$ $mole \cdot dm^{-2} \cdot s^{-1}$ is measured by these authors, which is in the range of what was found by Shoesmith and Sunder (1991).

⇒ Within the Spanish programme, Torrero et al. (1997) studied the oxygen promoted dissolution of unirradiated $UO_2(s)$ at three different oxygen partial pressures (5, 21 and 100% in nitrogen) and found a value of **n = 0.31** in the pH range from 3 to 6.7 in the absence of carbonate in the media. When working with carbonates, a dependence of 0.42 on the carbonate concentration was found (Torrero, 1995). At room temperature at 0.2 atm of oxygen and with a total carbonate concentration of 1 mM, a value of the rate of $8 \cdot 10^{-13}$ mole of $U \cdot dm^{-2} \cdot s^{-1}$ was measured, again in agreement with the observations of previous authors, Shoesmith and Sunder (1991) and Gray and Wilson (1995).

⇒ In an attempt to measure by spectrophotometry surface oxidation rates, Casas et al. (1994) report the variation of the U(VI) content on the surface of a unirradiated $UO_2(s)$ after variable contact times with a solution at pH = 8

under a partial oxygen pressure of 0.05 atm. By using these data and one additional experimental determination (de Pablo, pers. comm.) and by taking into account a density of uranium sites on the surface of the solid of $2.94 \cdot 10^{-5}$ mole$\cdot$dm^{-2} (Forsgren, 1988), it is possible to estimate an oxidation rate of $1.8 \cdot 10^{-11}$ moleU$\cdot$dm$^{-2}\cdot$s^{-1}.

It may be observed that the oxidation rate of UO_2 appears to be of two orders of magnitude larger than the rate of oxygen promoted dissolution obtained for most authors under similar circumstances. This could be an indication that the surface oxidation proceeds faster than the overall oxygen promoted dissolution which is a requirement for the overall oxidative dissolution reaction to proceed. However, we suspect that the actually reported uranium site density as obtained by Forsgren in his *examensarbete* at KTH could be larger than the typical density of surface sites obtained for most minerals, which varies between 2 and 20 sites per nm^2 (Davis and Kent, 1990). By using these lower site densities, we can estimate rates of oxidation ranging from $2 \cdot 10^{-14}$ and $2 \cdot 10^{-13}$ mole U$\cdot$dm$^{-2}\cdot$s^{-1}. The lower range would indicate that the rate determining step in the oxygen promoted dissolution is the actual surface oxidation, while in the upper range we obtain comparable values.

We summarise in Table 2-2 the kinetic information so far collected concerning the oxygen promoted dissolution of UO_2 phases, including uraninite minerals, unirradiated UO_2 and spent fuel.

Table 2-2. Summary of kinetic information on oxygen promoted dissolution of UO_2 phases.

Phase	T (°C)	pO_2 (atm)	pH	$[CO_3^{2-}]_{tot}$ (mole·dm^{-3})	R_{ox} (mole·dm^{-2}·s^{-1})	n	Reference
Uraninite	2 to 23	0.002 to 0.2	4 to 7	10^{-5} to 0.001	10^{-13} to 10^{-12}	1	Grandstaff (1976)
Uraninite	25	0.2 to 4	7.2 to 8	0.001 to 0.1	10^{-12} to 10^{-11}	0.5	Posey-Dowty et al. (1987)
CANDU Fuel	25	0.2	9.5	0	10^{-13}	1	Shoesmith and Sunder (1991)
CANDU Fuel	25	0 to 1	9.5	0 to 0.5		0.5 to 1	Hocking et al. (1992), Hocking et al. (1994)
UO_2 and Spent Fuel	25 to 75	10^{-6} to 0.2	8 to 10	0.02 to 0.04	10^{-13} to $2 \cdot 10^{-12}$	0.05 to 0.8	Gray et al. (1992), Gray and Wilson (1995)
UO_2	25	0.05 to 1	3 to 8	0 to 0.1	10^{-13} to 10^{-12}	0.3	Torrero (1995), Torrero et al. (1997)

From this Table it is possible to observe two main points: 1) the rate of oxygen promoted dissolution of UO_2 phases is of similar magnitude for all types of samples from synthetic uranium (IV) dioxide to spent nuclear fuel, including natural uraninites. 2) The rate order with respect to the dissolved oxygen ranges between 0.3 to 1 depending on the pO_2 considered in the experiments. At lower dissolved O_2 concentrations the order approaches linearity while fractional order rates for the oxygen promoted dissolution of UO_2 phases are obtained at higher pO_2.

This is a quite common phenomenon when studying the kinetics of heterogeneous processes. Stumm and co-workers (Stumm and Furrer, 1987) have proved that this is the indication that the attachment (sorption) of the reactive species (dissolved oxygen onto the UO_2 surface, in this case is the rate limiting step and that fractional reaction orders are obtained when approaching surface saturation by the active species. A comparable behaviour is obtained when studying the kinetics of the oxygen promoted dissolution of pyrite.

Moses et al. (1987) reported a linear dependence of the rate of oxidation of pyrite with the dissolved oxygen concentration when studying the kinetics of pyrite dissolution in aerated solutions. On the other hand, McKibben and Barnes (1986) report a 0.5 dependence when working in the pO_2 range 0.2 to 1 atm. Williamson and Rimstidt (1994) reported a reaction order of 0.5 with respect to dissolved oxygen when working over the pH range 2 to 10 and dissolved oxygen ranging from $2 \cdot 10^{-6}$ to $2 \cdot 10^{-2}$ mole$\cdot$kg^{-1}. This variable order of reaction can be explained in terms of a sorption mechanism by taking into account that prior to the electron transfer, the oxidant (in this case dissolved oxygen) must be sorbed to the surface. Nicholson et al. (1988) proposed a mechanism able to deal with this variation. According to these authors, the rate of oxidation R can be expressed by the following equation:

$$R = R_m \times K \times [O_2(aq)]/(1+K \times [O_2(aq)]) \qquad 2\text{-}15$$

where R_m is the rate based on maximum saturation of available surface sites and K is the adsorption equilibrium constant for oxygen on pyrite.

At low oxygen concentrations, the term $K \times [O_2(aq)]$ can be neglected in front of 1 and, therefore the rate is apparently first order with regard to the oxygen concentration in solution. When the term $K \times [O_2(aq)]$ is not negligible in front of 1, i.e., at larger oxygen concentration, the apparent order may vary between 0 an 1.

This type of equation, with arbitrary values given for R_m and K, is plotted in Figure 2-4. In that plot we can see that the apparent slope we would obtain depending on the range of oxygen concentrations can largely vary, from a minimum value of 0 at large $[O_2(aq]$ and a maximum value of 1 at low $[O_2(aq)]$. The points in the figure stand for the rates calculated by applying equation 2-15. If we work in the range of data where the stars apply and we try to fit a straight line to the data, a slope of 1 will be obtained and a good correlation is shown. The correlation is equally good if we work in the range where the circles apply, but in this case a slope of 0.5 is obtained. Finally, when working at the largest oxygen

concentrations show in the plot, the slope obtained, i.e., the order with respect to the oxygen content is 0.1 and the correlation is of the same goodness than in the two previous cases.

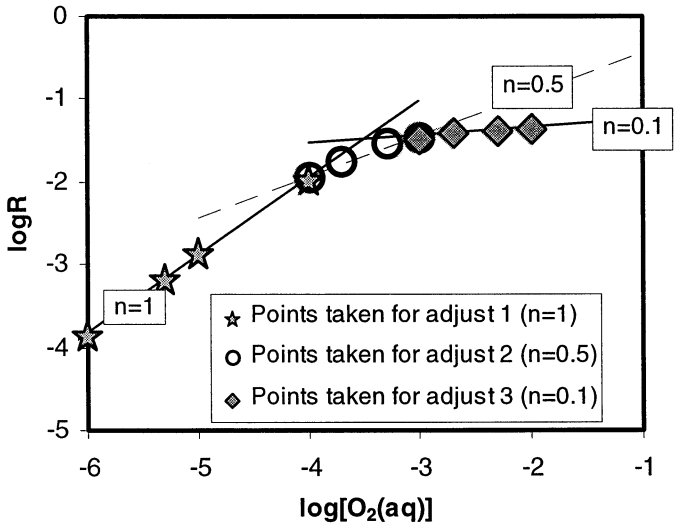

Figure 2-4. *Plot illustrating the different apparent orders with respect to the oxygen concentration that can be obtained from a rate law as the one expressed in equation 2-15.*

It is clear from this analysis than in the dissolved oxidant ranges expected in the repository conditions (10^{-6} to 10^{-8} mole·dm^{-3}), we will be far from surface saturation by the active species and consequently the reaction orders will approach linearity. However, when trying to explain the data obtained in contact with air we will have to take into consideration the fact that the UO_2 surface becomes saturated and that the oxygen promoted dissolution could show a fractional dependence.

Nevertheless, as we will see later the value of n will not have any important influence on the results obtained in the cases where a constant oxygen concentration was maintained throughout all the experimental time.

As said above, the selected conservative value for the oxidation rate has been the one estimated from XPS measurements by using a site density of $2.94 \cdot 10^{-5}$ moles of sites·dm^{-2}, i.e., $R_{ox} = 1.8 \cdot 10^{-11}$ mole U·dm^{-2}·s^{-1}. By taking into account that this value was obtained at room temperature under 0.05 atm of O_2(g), the following expressions for R_{ox} would be obtained in the case of assuming 0.5 or linear dependence on the [O_2(aq)]:

$$R_{ox} = 2.28 \cdot 10^{-9} \times [O_2(aq)]^{0.5} \text{ mole U·dm}^{-2}\text{·s}^{-1} \qquad 2\text{-}16$$

$$R_{ox} = 2.84 \cdot 10^{-7} \times [O_2(aq)] \text{ mole U·dm}^{-2}\text{·s}^{-1} \qquad 2\text{-}17$$

The former values would apply in the absence of carbonate in the media. According to Hocking et al. (1994), the presence of carbonate does not have any important influence on the order of the rate with respect to the oxygen

concentration and, therefore, we can assume that the same dependencies would apply to the rate law when carbonate are present.

By considering the data obtained by Gray and Wilson (1995) at 0.2 atm of O_2 under variable carbonate concentration, and the values of Torrero (1995) under the same conditions, an average value of :

$$R_{ox} = (1.3\pm0.5)\cdot10^{-11} \times [HCO_3^-]^{0.42} \text{ mole U}\cdot\text{dm}^{-2}\cdot\text{s}^{-1} \qquad 2\text{-}18$$

can be calculated. Therefore, the following two equations can be estimated under the presence of carbonate in the media:

$$R_{ox} = 8\cdot10^{-10} \times [O_2(aq)]^{0.5} \times [HCO_3^-]^{0.42} \text{ mole U}\cdot\text{dm}^{-2}\cdot\text{s}^{-1} \qquad 2\text{-}19$$

$$R_{ox} = 4.9\cdot10^{-8} \times [O_2(aq)] \times [HCO_3^-]^{0.42} \text{ mole U}\cdot\text{dm}^{-2}\cdot\text{s}^{-1} \qquad 2\text{-}20$$

Rate of dissolution of the oxidised spent fuel. Process 4 (R_{diss})

The dissolution process has been expressed by:

$$\begin{aligned} \left(> UO_2\right)_n \equiv U^{IV}_{0.667}U^{VI}_{0.334}O_{2.334} + 0.667H^+ \Rightarrow \\ \Rightarrow \left(> UO_2\right)_n \equiv \left(UO_2\right)_{0.667} + 0.334UO_2^{2+} + 0.334H_2O \end{aligned} \qquad 2\text{-}8$$

The only data available in this respect arises from well-controlled flow-through dissolution experiments of the $UO_{2.33}$ surface under nominally reducing conditions (Pd/H_2) (Bruno et al., 1991). From this work we selected the following value for the rate of dissolution of $UO_{2.33}$:

$$R_{diss} = (1.1\pm0.3)\cdot10^{-14} \times [H^+]^{-0.3} \text{ mole U}\cdot\text{dm}^{-2}\cdot\text{s}^{-1} \qquad 2\text{-}21$$

2.3 MATHEMATICAL DESCRIPTION OF THE MODEL

The mathematical description of the model is based on mass balance equations for each of the components involved in the system: oxidants (O_2 and H_2O_2), uranium, and the number of oxidised and non-oxidised sites at the spent fuel surface.

2.3.1 Oxidant evolution

The mass balance equation that would account for the evolution of the oxidant concentration in any hypothetical case, by considering radiolytic generation of oxidants will be expressed by the following equation:

$$[O_2]_t = [O_2]_{rad} - [O_2]_{ox} \qquad 2\text{-}22$$

where $[O_2]_{rad}$ stands for the generation of oxidants due to alpha-radiolysis of water, and $[O_2]_{ox}$ represents the consumption of oxidants due to the oxidation of

the spent fuel surface. The differential equation accounting for the evolution of $[O_2]$ will be:

$$\frac{d[O_2]_t}{dt} = R_{rad} - 0.167 \times R_{ox} \qquad 2\text{-}23$$

Most of the experiments on the dissolution of unirradiated $UO_2(s)$, were performed either in open systems in contact with air or where the oxidant concentration in the system was kept constant by bubbling $O_2(g)$ through the solution. In such cases, no mass balance equation is needed for the oxidant evolution.

One set of experiments was specifically designed to study the evolution of the radiolytically generated oxidants with time (Eriksen et al., 1995). In this case the evolution of oxidants in the system is known because there are direct measurements of the concentrations of O_2 and of H_2O_2, therefore, mass balance equations are not strictly required for this case, although necessary for the long-term projections.

Spent Fuel dissolution experiments performed at Studsvik (Forsyth *et al.*, 1986) were carried out in contact with air but in a nominally closed system. Therefore the evolution of the oxygen with time has to be calculated.

Although radiolytic generation of oxidants will occur under these conditions, the measured maximum oxidant concentration is in the level of $2 \cdot 10^{-5}$ to $2 \cdot 10^{-6}$ mole·dm^{-3} of dissolved oxygen (Eriksen et al., 1995). This is negligible compared with the initial dissolved oxygen present in the solution as a result of its contact with air ($2.48 \cdot 10^{-4}$ mole·dm^{-3}). Hence, in most cases the effect of air oxidation supersedes the actual radiolytic oxidation. Consequently the evolution of oxygen with time will be given by the consumption of the initially dissolved oxygen (in nominal equilibrium with air) by the oxidation of the spent fuel matrix in the closed system.

In this case, the calculations have been performed by assuming an initial O_2 concentration in the system in equilibrium with air (0.21 atm O_2) and that the rate of oxidant consumption will be equal to the rate of oxidation of the spent fuel. Hence:

$$\frac{d[O_2]}{dt} = -0.167 \times k_{ox} \times [O_2]^{0.5} \qquad 2\text{-}24$$

and, integrating from $[O_2]_0=2.48 \cdot 10^{-4}$ to $[O_2]=0$ and from t=0 to t, we obtain that the initial oxygen amount in contact with will be consumed at t=2200 days in the case of considering the experiments performed in bidistilled water, if no additional supply of oxygen is provided.

In the case of assuming linear dependence on the O_2 concentration, the following equation accounts for the O_2 consumption:

$$\frac{d[O_2]}{dt} = -0.167 \times k_{ox} \times [O_2] \qquad 2\text{-}25$$

and the time needed to consume all the oxygen initially present in solution largely increases.

As we have discussed in the previous section, probably what really happens is that at the initial high oxygen levels the order rate is fractional, but as dissolved oxygen levels decrease under a certain threshold (around 10^{-6} mole dm^{-3} could be a reasonable guess), then the dissolved oxygen is consumed linearly with time.

2.3.2 Uranium evolution

The evolution of the concentration of uranium in the system is strongly dependent on the physical design of the experimental system. Most of the experiments reported in the literature have been performed under batch conditions and, the oversaturation of the solution with respect to secondary uranium solid phases plays an important role. Furthermore, the flow conditions in an undisturbed spent fuel repository are expected to be *quasistatic,* with very low flow velocities (SKB-91, 1992). For this reason, although the kinetic model that we have developed takes into account the possibility of no oversaturation with respect to U(VI) secondary phases, it is clear that the conditions in the repository will favour the precipitation of secondary phases.

Study of the evolution of the system by neglecting the precipitation of secondary U(VI) solid phases due to oversaturation effects

In this case, the concentration of uranium in the system will continuously increase since no loss from the system occurs. The mass balance equation that will account for the uranium concentration at any time *t* will be expressed by the following equation:

$$[\mathrm{U(VI)}]_t = [\mathrm{U(VI)}]_{t-\Delta t} + \mathrm{R}_{diss} \times \Delta t \qquad 2\text{-}26$$

Study of the evolution of the system by assuming the precipitation of secondary U(VI) solid phases

There are two potential ways to approach the precipitation of secondary phases: either by assuming that the precipitation occurs instantaneously when secondary phase saturation conditions are reached, or by assuming that the oxidative dissolution of the matrix is retarded when saturation with respect to the secondary phases is approached. We will discuss the two cases separately.

Precipitation of secondary U(VI) solid phases according to equilibrium.

This approach assumes instant precipitation as soon as the concentration of uranium in solution reaches the value of saturation of an U(VI) solid phase, we

have considered this phase to be schoepite according to the experimental results. The set of equations describing this case will be:

$$[U(VI)]_t = \begin{cases} [U(VI)]_{t-\Delta t} + R_{diss} \times \Delta t\,; & \text{for } [U(VI)]_t < [U(VI)]_{eq} \\ [U(VI)]_{eq}\,; & \text{for } [U(VI)]_t \geq [U(VI)]_{eq} \end{cases} \qquad 2\text{-}27$$

Precipitation of secondary U(VI) solid phases retarded.

The most realistic approach to the evolution of uranium in solution had been to consider that the precipitation of secondary phases is not instantaneous but incorporates the well known fact that the precipitation of secondary phases is retarded and a certain degree of oversaturation occurs. This approach assumes that the precipitation of secondary U(VI) solid phases is governed by kinetics following the well-established Transition State Theory (Lasaga et al., 1994), and incorporates a retardation factor which depends on the saturation state of the system with respect to the solid phase that is precipitating.

However, this approach has not been considered in our calculations due to the lack of reliable rate constants for the dissolution and/or precipitation of schoepite.

3. TESTING OF THE MODEL AGAINST EXPERIMENTAL DATA

Once the processes and parameters are selected and the mathematical expressions are set, it is necessary to calibrate the model against a range of experimental data. Several published experimental results have been used for this purpose. The experimental data used for the calibrating exercise have been taken from the following sources:

3.1 UO_2 DISSOLUTION EXPERIMENTS WITH A CONSTANT OXIDANT CONCENTRATION IN THE SYSTEM (OPEN AIR SYSTEMS)

⇒ Ollila, (1995). These are experiments designed to obtain a rate of dissolution of $UO_2(s)$ under different experimental conditions. The $O_2(g)$ partial pressure was kept constant at the atmospheric value and two different media were used:

* Bidistilled water, at pH=5.8, with a Surface Area/Volume ratio of 59 dm^{-1}.

* Allard groundwater, with $[HCO_3^-]=2\cdot10^{-3}$ mole·dm^{-3}, at pH=8, with the same SA/V ratio.

3.2 SPENT FUEL DISSOLUTION EXPERIMENTS WITH VARIABLE OXIDANT CONCENTRATION IN THE SYSTEM

⇒ Forsyth et al., 1986. Experiments designed to obtain radionuclide release rates from spent fuel leaching tests:

* The evolution of the uranium concentration with time was measured in a medium containing $2\cdot10^{-3}$ mole·dm^{-3} HCO_3^- at pH=8. The initial $O_2(g)$ partial pressure was at the atmospheric value. SA/V=2.8 dm^{-1}.

* The evolution of the uranium concentration was measured in bidistilled water at pH=8. The initial $O_2(g)$ partial pressure was at the atmospheric value. SA/V=2.8 dm^{-1}.

⇒ Eriksen et al., 1995. Experiments designed to obtain the rate of oxidant generation by radiolysis of water. The experimental conditions were as follows:

* 1.88 g of spent fuel were put in contact with 0.014 dm^3 of water at pH=7. The evolution of the oxidant concentration with time was monitored (O_2 and

H_2O_2). At the end of the experiment, the concentration of uranium in solution was measured.

In spite of the fact that the experiments performed by Forsyth et al. (1986) were actually conducted using spent fuel therefore, under the influence of radiolytic effects, according to our previous discussion (section 2.3.1), we have considered that the evolution of the oxidant concentration with time is given by the consumption of the initial dissolved oxygen in the leaching solution, as the experiments were carried out in closed system conditions.

3.3 MODEL CALIBRATION RESULTS

3.3.1 Ollila (1995), UO_2 dissolution experiments performed in bidistilled water at pH=5.8.

Experimental conditions: SA/V=59 dm^{-1} and $pO_2(g)$=0.2 atm.

At this pH and without carbonates in the media, the major U(VI) aqueous species is UO_2OH^+.

The parameters introduced in the model are as follows:

- $R_{ox} = 2.28 \cdot 10^{-9} \times [O_2]^{0.5}$ mole·dm^{-2}·s^{-1} if we assume fractional order rate for the oxygen promoted dissolution of UO_2 (eq. 2-16).

- $R_{diss} = 6.04 \cdot 10^{-13}$ mole·dm^{-2}·s^{-1} (R_{diss} calculated at pH =5.8 from eq. 2-21).

- Solubility of "$UO_2(OH)_2$(s)" under the experimental conditions: $5.81 \cdot 10^{-6}$ mole·dm^{-3} (as calculated with the HARPHRQ code (Brown et al., 1991) by using the NEA database (Grenthe et al., 1992).

The results obtained from the application of the kinetic model are shown in Figure 3-1 compared to the experimental data. We can observe that the model calculations considering precipitation according to equilibrium reproduces the data fairly well. On the contrary, model calculations neglecting the precipitation of secondary phases predict much larger uranium concentrations than the ones actually measured.

In the case of assuming rate order one in the oxygen promoted dissolution of UO_2 we obtain:

$R_{ox} = 2.84 \cdot 10^{-7} \times [O_2]$ mole·dm^{-2}·s^{-1} (eq. 2-17),

and the results of the calculations are presented in Figure 3-2.

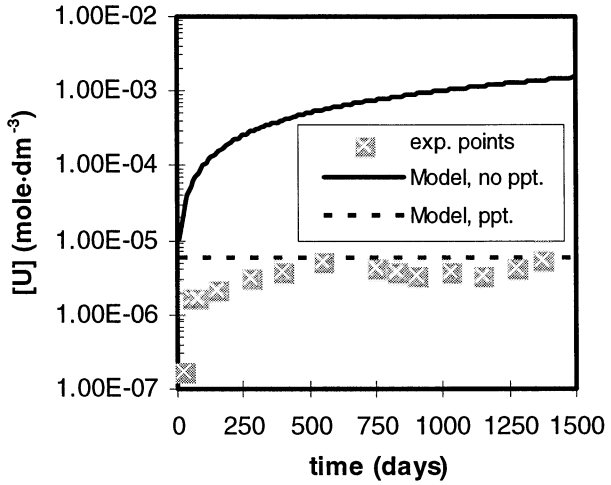

Figure 3-1. *Comparison between the experimental results from Ollila in bidistilled water and the results calculated with the model by assuming 0.5 rate order for the oxygen promoted dissolution of UO_2.*

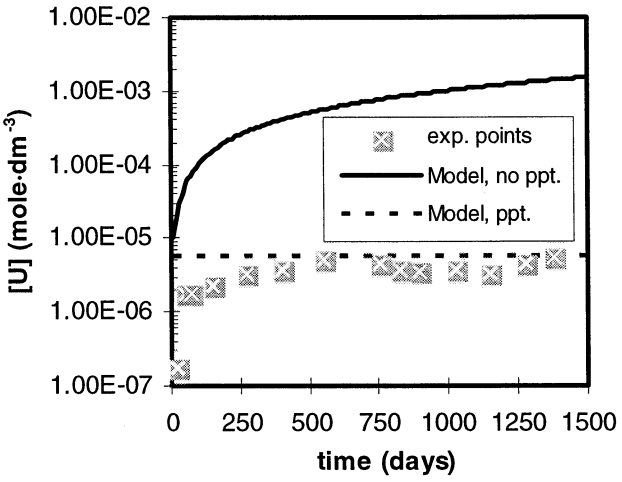

Figure 3-2. *Comparison between the experimental results from Ollila in bidistilled water and the results calculated with the model by assuming rate order one for the oxygen promoted dissolution of UO_2.*

As in the previous case, the model that considers precipitation according to equilibrium reproduces fairly well the experimental data.

Comparing the results in both figures (Figures 3-1 and 3-2) we can see that the model is not sensitive to consider a fractional or a linear oxygen dependence during these experimental times (up to 5 years). These experiments were performed by maintaining a constant oxygen partial pressure equal to 0.2 atm during all the time. Under these conditions, the dissolution of the oxidised uranium (VI) (eq. 2-21) is the process that limits the release of this radionuclide to the system, as the oxidation of the UO_2 surface is ensured by the constant and high supply of oxidants.

3.3.2 Ollila (1995), UO_2 dissolution experiments performed in Allard groundwater at pH=8.

Experimental conditions: SA/V=59 dm^{-1}, $[HCO_3^-]$=0.002 $mole \cdot dm^{-3}$ and $pO_2(g)$=0.2 atm.

At this pH and in the presence of carbonate, the major U(VI) aqueous species is $UO_2(CO_3)_2^{2-}$.

The parameters introduced in the model are as follows:

- $R_{ox}=8 \cdot 10^{-10} \times [O_2]^{0.5} \times [HCO_3^-]^{0.42}$ $mole \cdot dm^{-2} \cdot s^{-1}$ (R_{ox} value in bicarbonate media calculated at the actual dissolved oxygen and bicarbonate concentrations, eq. 2-19).

- $R_{diss}=2.76 \cdot 10^{-12}$ $mole \cdot dm^{-2} \cdot s^{-1}$ (R_{diss} calculated at pH = 8, from eq.2-21).

- Solubility of "$UO_2(OH)_2(s)$" under the experimental conditions: $9.3 \cdot 10^{-5}$ $mole \cdot dm^{-3}$ (calculated with the HARPHRQ code, by using the NEA database).

The results obtained from the application of the kinetic model are shown in Figure 3-3 in front of the experimental data.

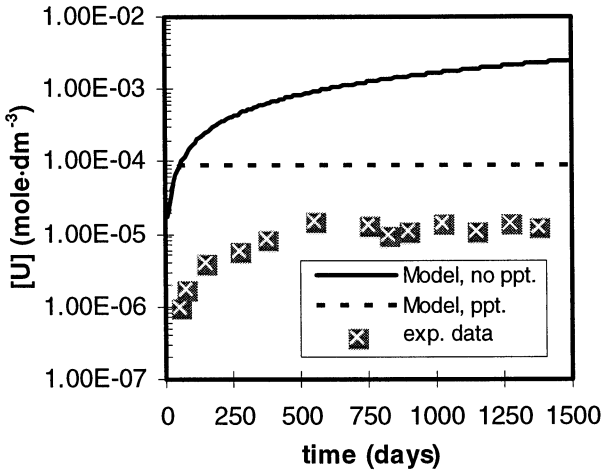

Figure 3-3. *Comparison between the experimental results from Ollila in Allard groundwater and the results calculated with the model by assuming rate order 0.5 for the oxygen promoted dissolution of UO_2.*

In this case, the model does not reproduce the measurements and it overpredicts the dissolved U(VI) concentrations.

Proceeding as in the previous case, assuming instead a linear dependence of the oxidation rate on the oxygen concentration, the expression for the oxidation rate will be:

$R_{ox}=4.9\cdot10^{-8} \times [O_2] \times\cdot[HCO_3^-]^{0.42}$ mole·dm^{-2}·s^{-1} (R_{ox} value in bicarbonate media by introducing the oxygen dependence, equation 2-20).

The results obtained are shown in Figure 3-4.

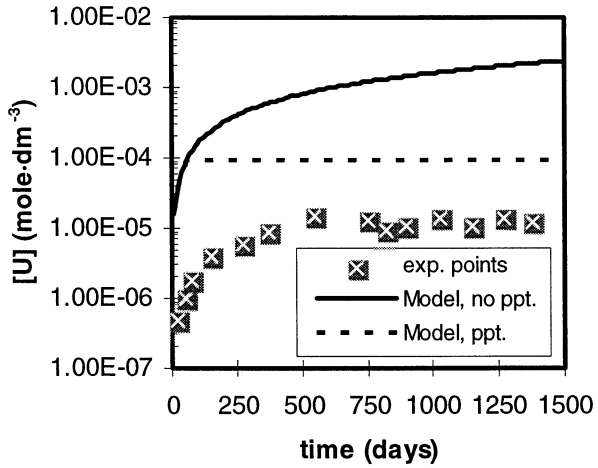

Figure 3-4. *Comparison between the experimental results from Ollila in Allard groundwater and the results calculated with the model by assuming rate order one for the oxygen promoted dissolution of UO_2.*

As in the previous case, the model does not fit the experimental data. The sensitivity analysis indicate that for unirradiated UO_2, in granitic groundwater the model is not sensitive to the assumption regarding linear and fractional dissolved oxygen dependence.

According to the model, under these experimental conditions, the oxidation of the UO_2 surface layer (eq. 2-19 or 2-20) is the process that limits the release of this radionuclide to the system.

This result agrees with the XPS observations of Torrero (1995). This author performed dissolution experiments with unirradiated UO_2 samples in carbonate solutions and in contact with air. In these experiments, the formation of the oxidised surface layer on the surface of the samples was not observed. This result indicates that the overall process was limited by the oxidation step. The high stability of the uranium-carbonate aqueous complexes in solution leads to a release of the uranium to the solution at the same rate as it is oxidised.

However, the bad fit of the model calculations to the actual dissolution data indicates that the assumed oxidation rate in bicarbonate media is too large. Consequently, and in order to fit Ollila's data, we have decreased the oxidation rate constants from equations 2-19 and 2-20, both by assuming fractional and linear dependence respectively. The oxidation rate constants assumed have been $k_{ox} = 8\cdot10^{-12}$ (from eq. 2-19) and $k_{ox} = 4.9\cdot10^{-10}$ (from eq. 2-20), R_{ox} in both cases expressed in mole·dm^{-2}·s^{-1}. The result to decrease these rate constants is given in Figure 3-5.

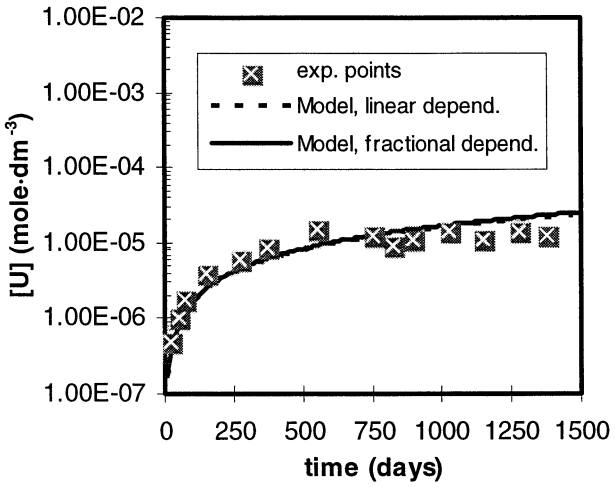

Figure 3-5. *Comparison between the experimental results from Ollila in Allard groundwater and the results calculated with the model, without precipitation. Linear and fractional dependence of the oxidation rate on the oxygen concentration (see text).*

Once the correction in R_{ox} is made, the model fits satisfactorily the experimental data. This newly indicates that in the presence of bicarbonate the surface oxidation is the rate limiting step but this proceeds at lower speed than expected.

3.3.3 Forsyth et al. (1986). Experiments in bidistilled water at pH=8.

Experimental conditions: SA/V=2.8 dm^{-1} and initial $pO_2(g)$=0.2 atm. At this pH and without carbonates in the media, the major U(VI) aqueous species is $UO_2(OH)_2$.

The parameters introduced in the model are as follows:

- $R_{ox}=2.28\cdot10^{-9}\times[O_2]^{0.5}$ mole·dm^{-2}·s^{-1} (eq. 2-18).
- $R_{diss}=2.76\cdot10^{-12}$ mole·dm^{-2}·s^{-1} (R_{diss} calculated at pH=8; from eq. 2-21).
- Solubility of "$UO_2(OH)_2$(s)" under the experimental conditions: $3.34\cdot10^{-7}$ mole·dm^{-3} (calculated with the HARPHRQ code, by using the NEA database).

The results obtained from the application of the kinetic model are shown in Figure 3-6 in front of the experimental data.

Due to the large scattering of the experimental data, the observed concentrations are reported as an experimental range.

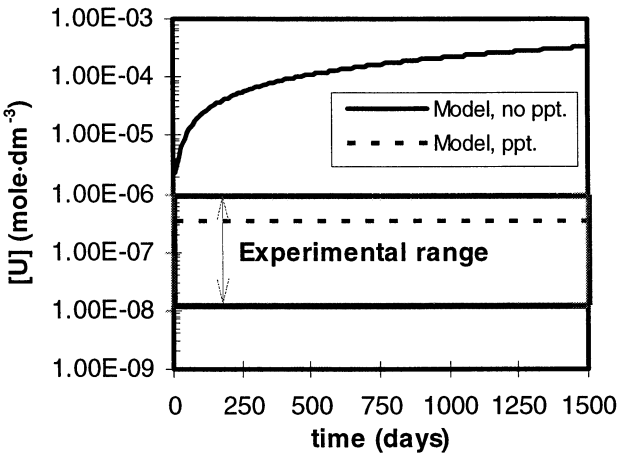

Figure 3-6. *Comparison between the experimental results from Forsyth et al. in bidistilled water and the results calculated with the model by assuming rate order 0.5 for the oxygen promoted dissolution of UO_2.*

Under these experimental conditions, the process limiting the release of uranium to the system is the dissolution of the oxidised surface layer (eq. 2-21) as the oxidation of the UO_2 surface is ensured by the high oxidant concentration in the system during the experimental time.

No sensitivity analysis of the effect of linear or 0.5 dependence of oxidation rate in dissolved oxygen is done, due to the insensitivity of the data. However, the model that assumes instant precipitation according to equilibrium is the one that best reproduces the results. This is probably due to the fact that the absence of complexing ligands makes secondary U(VI) precipitation quasi-instantaneous.

3.3.4 Forsyth et al. (1986). Experiments in bicarbonate media at pH=8.

Experimental conditions: $[HCO_3^-]=0.002 \cdot mole \cdot dm^{-3}$, initial $pO_2(g)=0.2$ atm. and $SA/V=2.8\ dm^{-1}$. At this pH and with carbonate in the media, the major U(VI) aqueous species is $UO_2(CO_3)_2^{2-}$.

The parameters introduced in the model are the same than in the previous case (Ollila, 1995 in Allard groundwater) due to the similarity of the experimental conditions, but they have been corrected with the SA/V ratio. The results obtained from the application of the kinetic model are shown in Figure 3-6 in front of the experimental data.

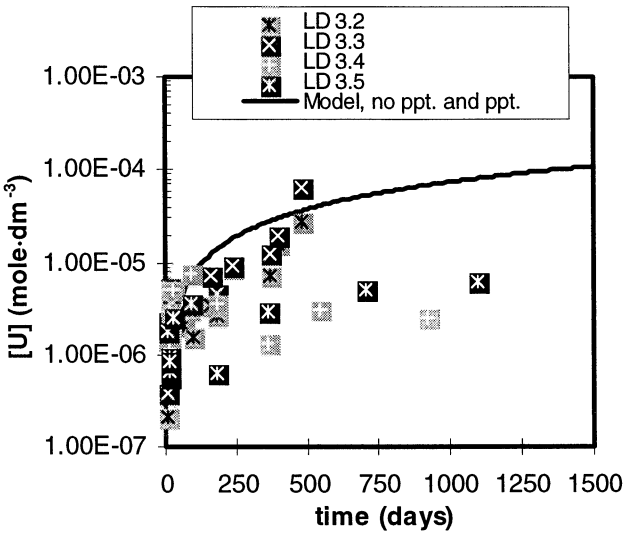

Figure 3-6. *Comparison between the experimental results from Forsyth et al. in bicarbonate media and the results calculated with the model by assuming rate order 0.5 for the oxygen promoted dissolution of UO_2. The symbols represent the different experiments that were run under the same conditions.*

If we assume linear dependence of the oxidation rate on the concentration of oxygen present in the system, the results showed in Figure 3-7 are obtained.

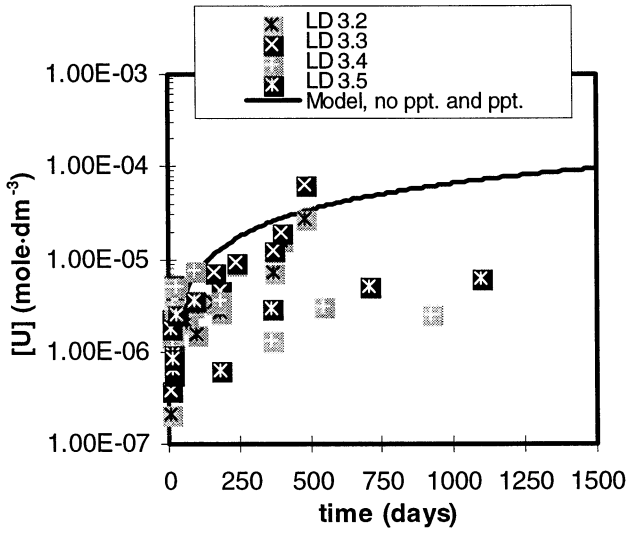

Figure 3-7. *Comparison between the experimental results from Forsyth et al. in bicarbonate media and the results calculated with the model by assuming rate order one for the oxygen promoted dissolution of UO_2.*

As we can see in the previous figures, the model fits quite well the experimental data, being the UO_2 surface oxidation the process that controls the release of uranium to the system under these experimental conditions.

According to the analysis performed, this system is sensitive to the effect of consider a linear or a fractional oxygen dependence only at contact times up to 1000 days approximately (Figure 3-8), due to the fact that the oxygen concentration decreases with time. However, these times are larger than the experimental ones.

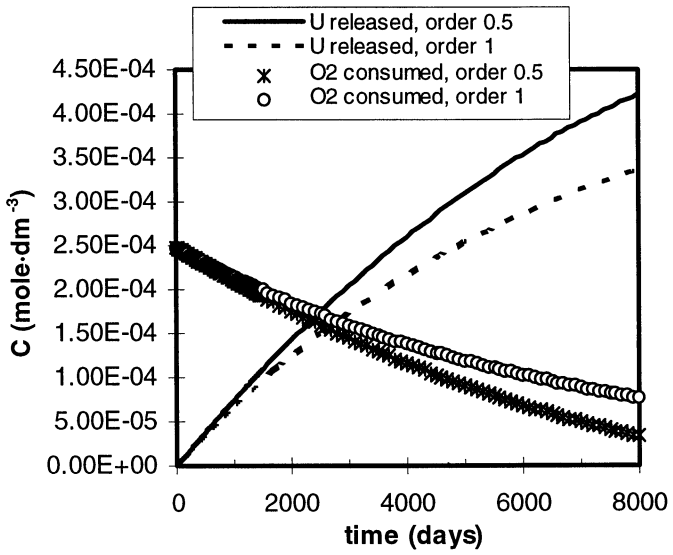

Figure 3-8. *Model calculations of the uranium released and the oxygen remaining in the system by assuming rate order 0.5 and one for the oxygen promoted dissolution of UO_2, under the experimental conditions of Forsyth et al. in Allard ground water.*

Finally, we have calculated the evolution of the uranium concentration with time by taking the oxidation rate constants previously selected in order to fit Ollila's dissolution data (section 3.3.2). The results indicate that the model does not fit the actual experimental data when decreasing the oxidation rate in the same extent as for Ollila's results.

This fact would indicate that there is still some remaining uncertainty concerning the magnitude (approximately of one order) and mechanism of the combined effect of oxygen and bicarbonate promoted UO_2 dissolution.

3.3.5 Eriksen et al. (1995). Experiments performed in bidistilled water at pH=7.

Experimental conditions: SA/V=161 dm^{-1}; $pO_2(g)$ not constant, measured with time.

At this pH and without carbonates in the media, the major U(VI) aqueous species is $UO_2(OH)_2$.

The parameters introduced in the model are as follows:

- $R_{ox}=2.28\cdot10^{-9} \times [O_2]^{0.5}$ mole·$dm^{-2}\cdot s^{-1}$ (eq. 2-16).

- $R_{diss}=1.38\cdot10^{-12}$ mole·dm^{-2}·s^{-1} (R_{diss} calculated at pH 7 from eq. 2-23).

- Solubility of "$UO_2(OH)_2(s)$" under the experimental conditions: $4.67\cdot10^{-7}$ mole·dm^{-3} (calculated with the HARPHRQ code, by using the NEA database).

The results obtained from the application of the kinetic model are shown in Figure 3-9 in front of the experimental data.

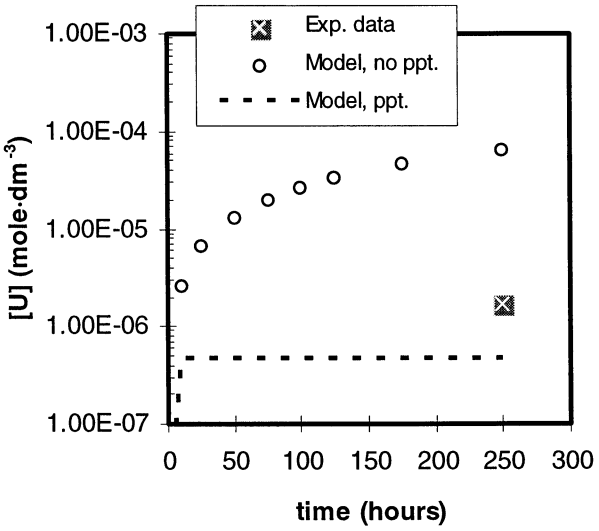

Figure 3-9. *Comparison between the experimental result from Eriksen et al. in bidistilled water and the results calculated with the model. Fractional oxygen dependence on the oxidation rate.*

By applying the linear oxygen dependence on the oxidation rate with a rate constant of k_{ox} = $2.84\cdot10^{-7}$ dm·s^{-1} (from eq. 2-17) we obtain the results given in Figure 3-10.

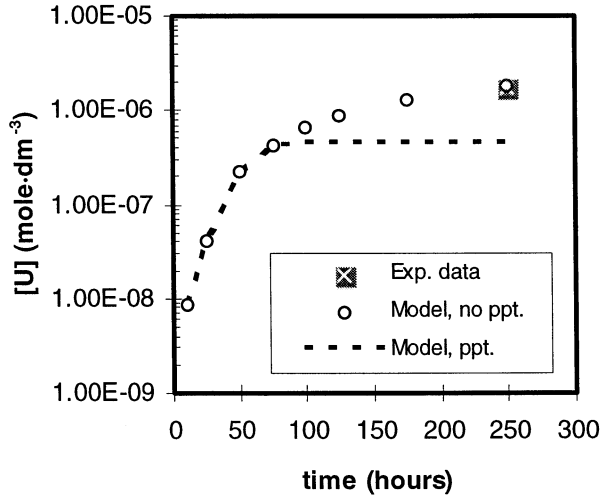

Figure 3-10. *Comparison between the experimental result from Eriksen et al. in bidistilled water and the results calculated with the model. Linear oxygen dependence on the oxidation rate.*

From the previous figures (Figures 3-9 and 3-10) we can see that this system is very sensitive to the oxygen dependence of the oxidation rate and therefore, it constitutes a potential way to differentiate among the reaction rate orders for the oxygen promoted dissolution of UO_2.

As a consequence of the experimental set-up (Eriksen et al., 1995), the oxygen present in this system is exclusively generated by the radiolysis of water. The oxygen concentrations measured range between $2 \cdot 10^{-6}$ and $2 \cdot 10^{-5}$ mole·dm^{-3}. These oxygen concentrations are low in comparison with the oxygen concentrations calculated in the previous analyses (sections 3.3.1 and 3.3.3), with oxygen concentrations from $8 \cdot 10^{-5}$ to $2.5 \cdot 10^{-4}$ mole·dm^{-3}. At the oxygen levels measured in this work, the oxidation rate is the process limiting the release of uranium to the system.

At these low oxygen concentrations, the oxygen dependence on the oxidation rate plays an important role at early contact times. At larger oxygen concentrations, this dependence is only sensitive at longer contact times and in a closed system.

The good fit of the model to the experimental data by considering a linear oxygen dependence (Figure 3-10) is in agreement with our previous discussion. At low oxygen concentrations, the oxidation rate is first order with regard to the oxygen concentration in solution.

4. APPLICATION OF THE KINETIC MODEL TO OTHER MINOR RADIONUCLIDES

The results obtained from the modelling of the uranium dissolution behaviour by applying the mass balance kinetic model have been quite encouraging. Consequently, the next step of this work has been to assess to which extent the kinetic model for the stability of the spent fuel matrix can be extended to the minor radionuclides contained in the matrix.

For this purpose, three minor radionuclides, Pu, Tc and Sr, have been selected to apply the kinetic model previously developed.

The selection of these radionuclides has been carried out according to different criteria:

* Pu has been selected as a critical radionuclide when assessing the safety of the spent fuel disposal and because it is expected to behave chemically in a similar fashion to uranium.

* Tc is another critical radionuclide which is initially located as a separate phase in the fuel forming metallic inclusions.

* Finally, Sr has been selected since it has been proposed as a potential indicator of the dissolution of the spent fuel matrix.

The model has been tested against experimental results from spent fuel dissolution tests obtained within the SKB programme (Forsyth and Werme, 1992, Forsyth and Eklund, 1995). Only data obtained under oxic conditions and using synthetic granitic groundwater as solvent have been analysed. The data have been presented in terms of radionuclide concentration as a function of time.

This exercise has been very useful in identifying the different processes by which the release of every radionuclide is controlled. The following figure (Figure 4-1) shows the trend of the dissolution process for U, Pu, Tc and Sr as a function of time. In general, the initial spent fuel dissolution can be regarded as quasi congruent. However, at longer contact times, the behaviour of uranium and that of other radionuclides appears to be de-coupled, indicating that different processes are responsible for their final concentration in the solution contacting the fuel.

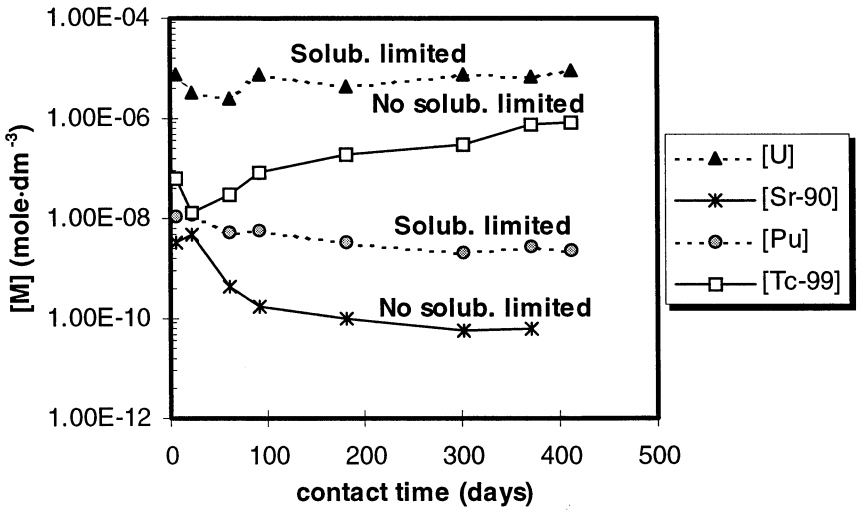

Figure 4-1. *U, Pu, Tc and Sr concentrations as a function of time.*

The kinetic model has been applied to the minor radionuclides by initially considering a congruent release with respect to the spent fuel UO_2 matrix, according to the inventory ratio. Therefore, the dissolved minor radionuclide (RN) concentration is considered to be equal to the uranium released times the molar fraction of this radionuclide in the fuel according to the inventory. This according to the general equation:

$$[RN]_t = \chi_{RN} \times [U]_t \qquad 4\text{-}1$$

4.1 PLUTONIUM

The general trend of the Pu dissolution data is given in the next figure (Figure 4-2).

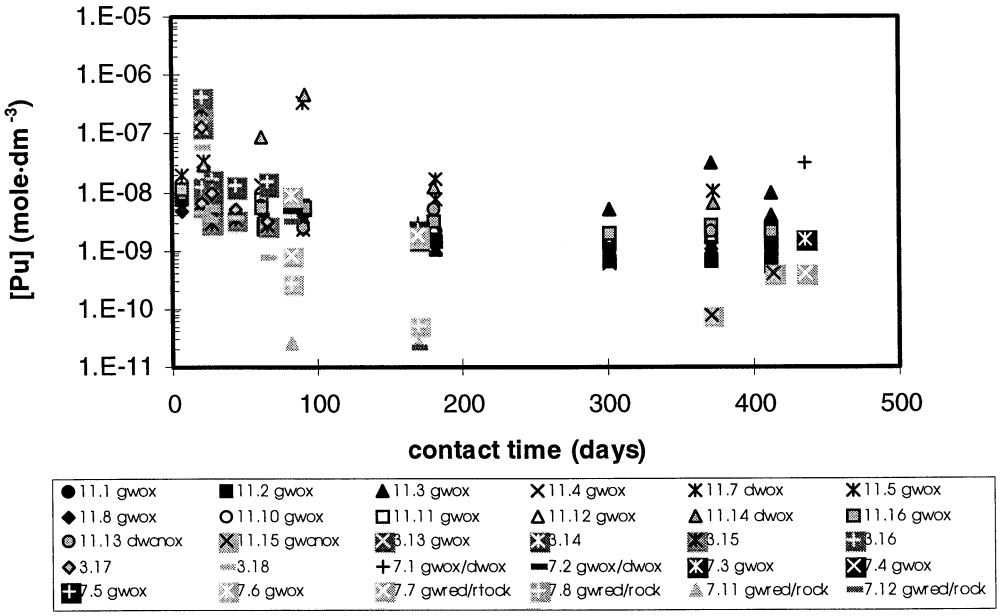

A)

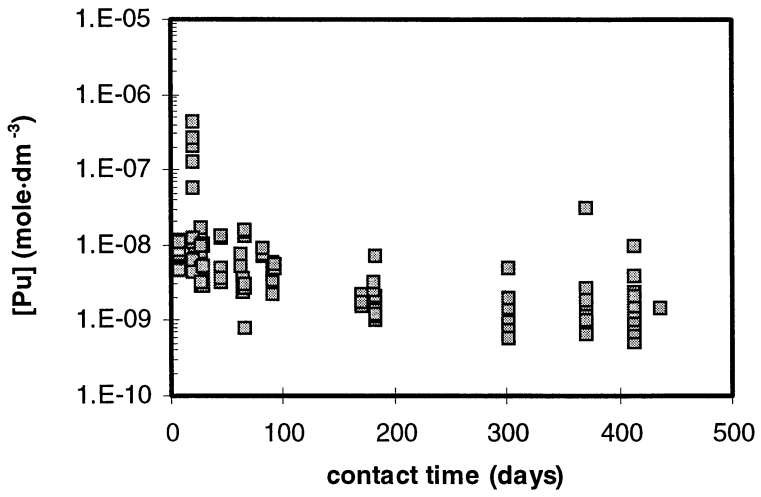

B)

Figure 4-2. *A) Plot of Pu released from spent fuel leaching experiments as a function of time. Experimental data corresponding to series 3, 7 and 11.* ***B)*** *Data under oxidising conditions and in groundwater media.*

As we can see in the Figure 4-2, the behaviour of the Pu release under oxidising conditions in groundwater media is as follows: At the first contact days of there is a sharp increase of the Pu concentrations in the solutions. Later on, the Pu concentrations slowly decrease to an apparently constant level. This behaviour may be an indication of two different processes occurring in the system. The initial release of Pu as the matrix dissolves, up to a certain level when the Pu concentration in solution is sufficiently large (approximately 10^{-8} mole dm^{-3}) to trigger the precipitation of a secondary phase. In granitic groundwaters, the Pu concentrations reach an steady state level in the range 10^{-9} to 10^{-10} mole·dm^{-3}.

Under the experimental conditions, Pu(IV) is the thermodynamically stable redox state both in the solid and aqueous phases. It is well known that Pu(IV) has a strong and worrisome tendency to build colloidal dispersions in contact with water. However, these colloids tend to aggregate towards the formation of $Pu(OH)_4(am)$ with time in electrolyte solutions. According to this, we can establish which would be the main processes to be considered, together with the kinetic and thermodynamic parameters to model the experimental data:

⇒ Congruent dissolution of Pu(IV) from the matrix to form the predominant Pu(IV) aqueous complex

$$xPuO_2 + 2x\ H_2O \Rightarrow xPu(OH)_4(aq) \qquad 4\text{-}2$$

where x stands for the mole fraction of Pu present in the UO_2 matrix, which basically depends on the burnup history, this value has been considered to range between 0.01 and 0.02 (SKI SITE 94, 1996).

Consequently, by assuming a congruent dissolution process, the rate will be given by the product of the x the mole fraction of Pu in the matrix, times the oxidative

dissolution rate of the UO_2 matrix. Therefore, by taking the rate of oxidation of the UO_2 matrix (see Chapter 2, section 2.2.2), we obtain:

$$R_0(Pu)=x \times R_{ox}(UO_2)=(0.5\text{-}1)\cdot 10^{-13} \text{ mole Pu}\cdot dm^{-3}\cdot s^{-1} \qquad 4\text{-}3$$

$\Rightarrow$ Build up of colloidal Pu(IV)

$$Pu(OH)_4(coll) \underset{k_{-1}}{\overset{k_1}{\rightleftharpoons}} Pu(OH)_4(aq) \qquad 4\text{-}4$$

This is a comparatively fast and apparently reversible process. Therefore, the overall dissolution process up to the formation of colloidal Pu(IV) is controlled by the dissolution kinetics of the Pu from the matrix.

The rate of dissolution for the previous reaction will be given by the following equation:

$$R_1 = k_1 - k_{-1} \times [Pu(OH)_4(aq)] \qquad 4\text{-}5$$

$\Rightarrow$ Ageing of the Pu(IV) to precipitate as $Pu(OH)_4(am)$

$$Pu(OH)_4(aq) \underset{k_{-2}}{\overset{k_2}{\rightleftharpoons}} Pu(OH)_4(am) \qquad 4\text{-}6$$

Puigdomènech and Bruno (1991) reported a logK=9.98 for the previous equilibrium (eq. 4-5). This constant gives a final steady state concentration of $1.03\cdot 10^{-10}$ mole$\cdot dm^{-3}$ of Pu(IV) in equilibrium with $Pu(OH)_4(am)$ under the experimental conditions. This value is in fairly good agreement with the long-term apparent Pu solubilities measured in groundwater.

The rate expression for the precipitation of the amorphous $Pu(OH)_4(am)$ from the aqueous $Pu(OH)_4(aq)$ will be given by the expression:

$$-R_2 = k_{-2} - k_2 \times [Pu(OH)_4(aq)] \qquad 4\text{-}7$$

Integrating equation 4-5 from [Pu]=0 to $[Pu]=[Pu]_0$ (Pu stands for $Pu(OH)_4(aq)$ in a simplified form) and from t=0 to t, we obtain the following equation, which accounts for the variation of the Pu concentration with time due to the dissolution of the colloids:

$$[Pu]_0 = \frac{k_1}{k_{-1}}\{1-\exp(-k_{-1}\times t\} \qquad 4\text{-}8$$

The precipitation of $Pu(OH)_4(am)$, eq. 4-6, will start from the Pu concentration released in the first process (4-4), therefore, we will integrate the former

expression from $[Pu]_0$ to [Pu] and from $t_0=0$ to t, where $[Pu]_0$ will be given by equation 4-8. The resulting evolution of the Pu concentration with time will be:

$$[Pu] = \frac{k_{-2}}{k_2} - \left\{\frac{k_{-2}}{k_2} - \frac{k_1}{k_{-1}}\{1-\exp(-k_{-1}\times t\}\right\} \exp\{-k_2\times t)\} \qquad 4\text{-}9$$

The ratio k_1/k_{-1} is equivalent to the equilibrium constant for the process in equation 4-4 (K_1), and the ratio k_{-2}/k_2 stands for the inverse of the equilibrium constant for the precipitation of $Pu(OH)_4(am)$ process ($1/K_2$), i.e., k_{-2}/k_2 will be equal to the solubility constant of the amorphous solid phase that is precipitating: $Pu(OH)_4(am)$, K_{so}.

Equation 4-9 was used to fit the experimental data, the results of the fitting are shown in Figure 4-3.

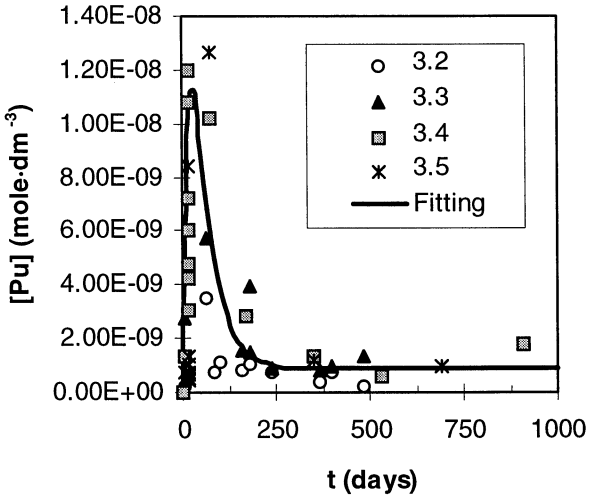

Figure 4-3. *Fitting of equation 4-9 to experimental data. Only series 3 have been plotted in this figure.*

The average parameters and the standard deviations obtained from the best fit of the experimental data are given in Table 4-1.

Table 4-1. Parameters obtained by fitting the experimental data.

	$\frac{k_1}{k_{-1}}$ (K_1)	$\frac{k_{-2}}{k_2}$ (K_{so})	k_{-1} (d^{-1})	k_2 (d^{-1})
Average	$2.8\cdot10^{-8}$	$8.75\cdot10^{-10}$	0.046	0.022
St.dev	$0.1\cdot10^{-8}$	$0.43\cdot10^{-10}$	0.016	0.008

From these parameters, we obtain the following equilibrium constants for the processes considered:

$$Pu(OH)_4(coll) \Leftrightarrow Pu(OH)_4(aq) \qquad 4\text{-}4$$

$$K_1=(2.8\pm0.1)\cdot10^{-8}$$

$$Pu(OH)_4(aq)\Leftrightarrow Pu(OH)_4(am) \qquad 4\text{-}6$$

$$K_2=1/(8.75\pm0.43)\cdot10^{-10}$$

and

$$K_{so}=(8.75\pm0.43)\cdot10^{-10}$$

The value of K_{so} is within one order of magnitude of the value reported by Puigdomènech and Bruno (1991). Both the good statistics of the fitting parameters and the reasonable agreement with independently determined thermodynamic data, gives us confidence in the process model proposed to explain the behaviour of Pu in spent fuel dissolution experiments. It has to be pointed out that $Pu(OH)_4(am)$ as the secondary Pu solid phase was already suggested by Forsyth and Werme (1992).

The solubility constant obtained for $Pu(OH)_4(coll)$ is 2 orders of magnitude larger than the corresponding to $Pu(OH)_4(am)$, as it is expected from its very disordered nature.

4.2 TECHNETIUM

The results of Tc dissolution data obtained from spent fuel leaching experiments in Studsvik are shown in Figure 4-4. In this figure it is possible to differentiate between the behaviour under oxidising and under nominally anoxic or reducing conditions. In this work, only the results under oxidising conditions will be studied.

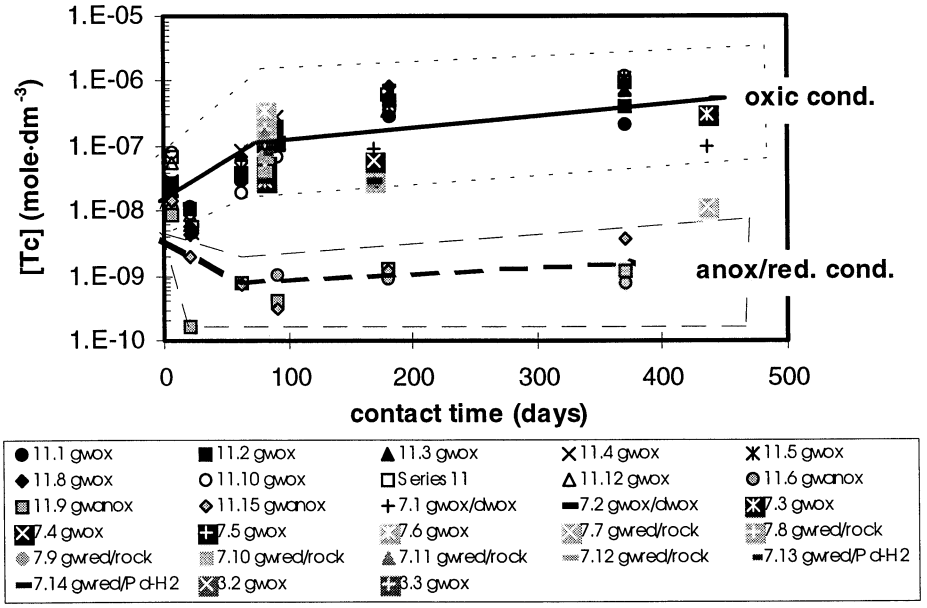

Figure 4-4. Plot of Tc released from spent fuel leaching experiments as a function of time. Experimental data corresponding to series 3, 7 and 11. Solid lines indicate the general trend of the data.

The solubility of this radionuclide under the experimental conditions, pH=8, $pO_2(g)$=0.2 atm and $[HCO_3^-]$=0.002 mole·dm^{-3}, is very high due to the stability of TcO_4^- under oxidant conditions (calculations performed with the EQ3NR code (Wolery, 1992), by using the NAGRA/SKB-97 TDB (Bruno et al., 1997b)). Therefore we can conclude that technetium is not solubility limited. (Figure 4-4).

Consequently, we have considered that technetium will co-dissolve with uranium according to the inventory ratio of the spent fuel samples used in the experiments. The mean inventory ratio is 0.002, and this is the value used in the calculations. The congruent Tc release rates are calculated according to eq. 4.1 The results are given in Figure 4-5.

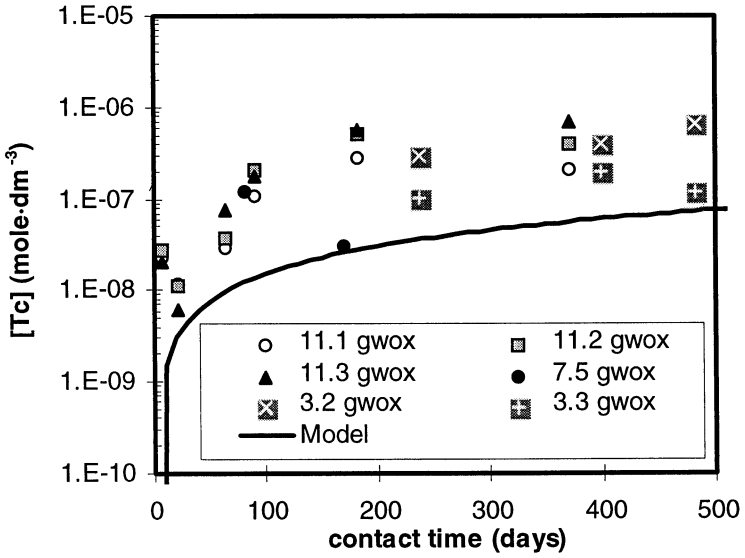

Figure 4-5. *Comparison between the model and the experimental data. For the sake of simplicity only some of the experimental results have been included in this figure.*

As we can see from the previous figure, the model reproduces quite well the data at short contact times (<50 days). However, at longer contact times the calculated technetium concentration is lower than the measured ones.

Only at early contact times, technetium is released congruently with uranium since its ratio in solution agrees with the initial inventory ratio of the fuel sample, as it is shown in Figure 4-6. Therefore, during this period the model reproduces the experimental data. At longer contact times, the ratio of Tc-99/U in solution is larger than the initial inventory ratio (Figure 4-6), therefore, a larger release of technetium with respect uranium occurs, for this reason technetium concentrations calculated are lower than measured, since congruent dissolution has been considered in the model during all the experimental time.

This de-coupling could be explained as a result of the uranium precipitation in secondary phases which do not incorporate the perthecnetate released. In this case, the solution would be enriched in technetium with respect to uranium with increasing time. However, our model calculations predict the precipitation of

uranium secondary phases at longer contact times (larger uranium (VI) concentrations) than the ones covered in these experiments.

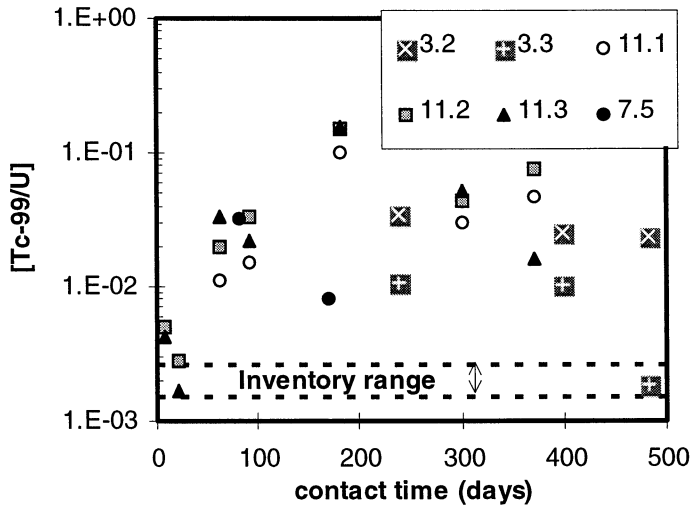

Figure 4-6. *Plot of the experimental data as a function of time. Dotted lines indicate the inventory range calculated from the spent fuel samples used in the dissolution tests.*

Nevertheless, the incongruent dissolution of technetium with respect to uranium at longer contact times indicates that both radionuclides have to be treated separately as different processes appear to control their release from the matrix.

4.3 STRONTIUM

The results on Sr dissolution data obtained from spent fuel leaching experiments in Studsvik are given in Figure 4-7.

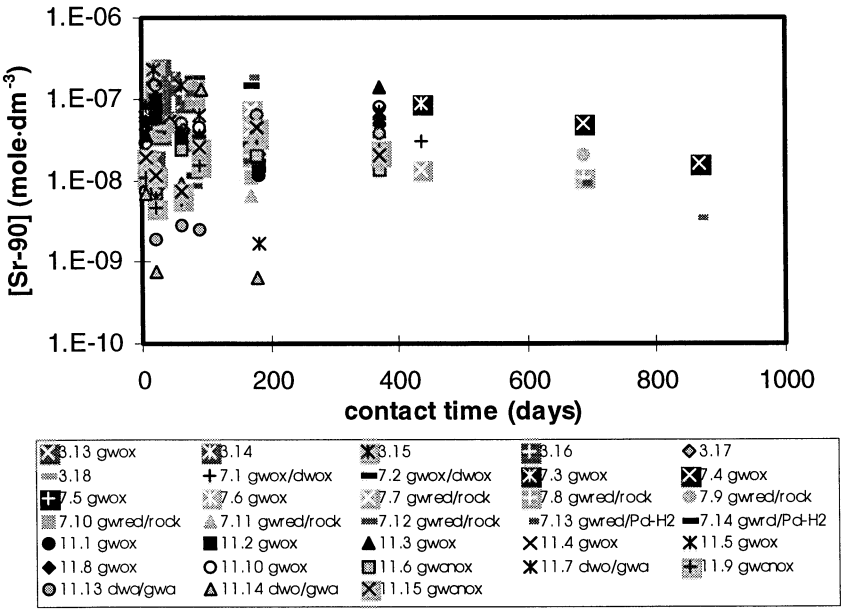

Figure 4-7. *Plot of Sr released from spent fuel leaching experiments as a function of time. Experimental data corresponding to series 3, 7 and 11.*

The solubility limiting solid phase under the experimental conditions is strontianite (calculations performed with the EQ3NR code package together with the NAGRA/SKB-97 TDB), its solubility is larger than the strontium concentration measured in the leaching solution (Figure 4-8). Therefore, we can conclude that strontium is not individually solubility limited, at least at the experimental contact times. Consequently another process will limit the concentration of this radionuclide in solution. For this reason we have taken into consideration a co-dissolution process of strontium with the UO_2 matrix according to the inventory ratio of the spent fuel samples used in the experiments. The mean inventory ratio considered has been 0.0015. The results of the calculations are given in Figure 4-8.

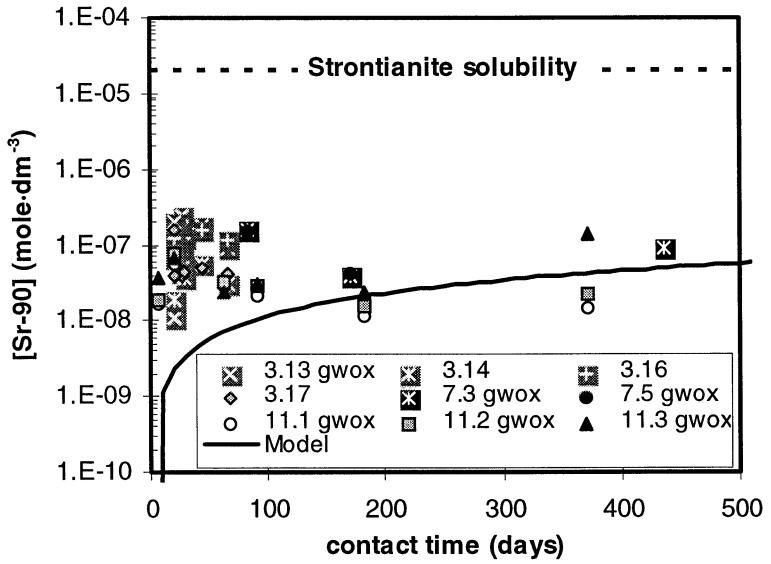

Figure 4-8. *Comparison between the model and the experimental data. For the sake of clarity not all the results have been plotted in this figure. Dotted line shows strontianite solubility under the experimental conditions.*

As we can see from the previous figure, the model reproduces quite well the data until 500 days approximately. This agreement indicates that a co-dissolution process with the UO_2 matrix could be expected for this radionuclide.

However, during the early contact times (<100 days), the release of strontium is faster than expected according to the co-dissolution process. This discrepancy can be explained by the fact that Sr-90 is enriched in the spent fuel grain boundary and, therefore, its initial release is larger than the one of uranium.

5. CONCLUSIONS AND SUGGESTIONS FOR FURTHER WORK

The work so far presented indicates that the combination of oxidant and reductant mass balances, together with the relevant kinetic information as contained in the model, constitutes a useful tool to bring some rationale to observations from both spectroscopic and chemical solution data concerning the dissolution behaviour of UO_2 phases (uraninites, unirradiated UO_2 and spent fuel), as well as specific experiments devised to quantify the oxidant and reductant generation at the spent fuel/water interface.

Concerning the status of the kinetic data required, our analysis indicates the following:

⇒ There is a need to a systematic and independent quantification of the density of UO_2 sites prone to oxidation. This parameter will allow a better estimation of the UO_2 surface oxidation rate calculated from XPS analyses.

⇒ There is a clear need for more precise experimental measurements for the rate and mechanisms of the hydrogen peroxide promoted dissolution of UO_2. These experiments should be performed in the hydrogen peroxide concentration range of relevance for the radiolytic oxidation of spent fuel ($<10^{-3}$ mole·dm^{-3}).

⇒ The rates and mechanisms for the oxygen promoted dissolution have been studied to a far more extent. However in most of the cases in pO_2 conditions which are much larger than the ones expected in the spent fuel disposal systems. Our analysis of the data indicates that the apparent controversies between the various reaction order rates as observed by different authors can be rationalised in terms of surface saturation with respect to the sorbed oxygen. A similar effect has been observed when studying the rates of oxidation of pyrite. Rates of oxidative dissolution obtained in contact with air do overestimate the actual rates expected in repository conditions, this is the actual oxygen concentration in contact with air is much larger than the ones expected from water radiolysis in anoxic media. It is our firm conviction that spent fuel leaching experiments in contact with air do not bring any additional information and in many cases they introduce some confusion, hence they should be discontinued.

⇒ In this context, the data so far analysed indicates that the rates of oxygen promoted dissolution of UO_2 are linear with respect to the dissolved oxygen concentration at the concentration ranges of relevance for spent fuel disposal ($[O_2(aq)]<10^{-5}$ mole·dm^{-3}).

⇒ The rates and mechanisms for the combined oxygen and bicarbonate promoted dissolution of UO_2 will require a further experimental definition, particularly in oxygen concentration ranges relevant to the disposal system.

Concerning, the status of applicability of the kinetic model to minor radionuclides the results so far obtained are quite encouraging.

Particularly, in the case of Pu, where the model presented appears to reproduce the behaviour of this critical radionuclide in experiments at early contact times.

In the case of Tc, there seems to be a differentiated mechanism for the release of this radionuclide with respect to the UO_2 dissolution. This would be expected from the chemical form and behaviour of this radionuclide in the spent fuel.

The long term dissolution behaviour of Sr appears to be congruent with UO_2 dissolution. However, at shorter contact times this radionuclide appears to be released at larger rates than expected from congruent dissolution from the spent fuel matrix. This could be explained by the fact that Sr is somewhat enriched at grain boundaries. The conciliation between these observations could give some settling to the controversy concerning the role of Sr as matrix dissolution marker.

6. REFERENCES

Allen G.C. and Tyler J.W., 1986. Surface Characterisation of β-U_3O_7 using X-ray photoelectron spectroscopy. J. Chem. Soc., Faraday Trans. 1, 82, 1367-1379.

Brown P.L., Haworth A., Sharland S.M., Tweed C.J., 1991. HARPHRQ: A geochemical speciation program based on PHREEQE. Theoretical Studies Department. Radwaste Disposal Division b424.2. Hornwall Laboratory, Didcot Oxon OX11ORA.

Bruno J., Casas I. and Puigdomènech I., 1991. The kinetics of dissolution of UO_2 under reducing conditions and the influence of an oxidized surface layer. Geochim. et Cosmochim. Acta 55, 647-658.

Bruno J., Casas I., Cera E., de Pablo I., Giménez J. and Torrero M.E., 1995. Uranium (IV) dioxide and SIMFUEL as chemical analogues of nuclear spent fuel matrix dissolution. A comparison of dissolution results in a standard $NaCl/NaHCO_3$ solution. Mater. Res. Soc. Symp. Proc. 353, 601-608.

Bruno J., Cera E., Duro L., Eriksen T.E. and Werme L.O., 1996. A kinetic model for the stability of spent fuel matrix under oxic conditions. J. Nucl. Mater. 238, 110-120.

Bruno J., Cera E., Duro L., Eriksen T.E. Sellin P. Spahiu K. and Werme L.O., 1997a. A kinetic model for the stability of the spent fuel matrix under oxic conditions. Model development against experimental evidence. Mater. Res. Soc. Symp. Proc. 465, 491-502.

Bruno J., Cera E., de Pablo J., Duro L., Jordana S. and Savage D., 1997. Determination of radionuclide solubility limits to be used in SR'97. Uncertainties associated to calculated solubilities. QuantiSci Internal Report, December 1997.

Bruno J. and Puigdomènech I., 1989. Validation of the SKBU1 uranium thermodynamic data base for its use in geochemical calculations with EQ3/6. Mater Res. Soc. Symp. Proc. 127, 887-896.

Casas I., Giménez J., Martí V., Torrero M.E. and de Pablo J., 1994. Kinetic studies of unirradiated UO_2 dissolution under oxidizing conditions in batch and flow experiments Radiochim. Acta, 66/67, 23-27.

Casas I., Sandino A., Caceci M.S., Bruno J. and Ollila K., 1991. SIMFUEL Dissolution Studies in Granitic Groundwater. SKB Technical Report TR 91-34.

Christensen H., 1990. Calculation of the effect of alpha-radiolysis on UO_2 oxidation. Studsvik Nuclear. Rapport nr. NS-90/72.

Christensen H., 1991. Radiation induced dissolution of UO_2. Mater Res. Soc. Symp. Proc. 212, 213-220.

Christensen H., Sunder S. and Shoesmith D.W., 1994. Oxidation of nuclear fuel (UO_2) by the products of water radiolysis: development of a kinetic model. J. of Alloys and Compounds, 213/214, 93-99.

Davis J.A. and Kent D.B., 1990. Surface complexation modeling in aqueous geochemistry, in: Mineral-Water Interface Geochemistry, Rev. Mineral., Vol. 23 (M.F. Hochella and A.F.White ed.) Mineral. Soc. Am. Washington D.C., 177-260.

Eriksen T.E., 1996. Radiolysis of water within a ruptured fuel element. SKB Progress Report U-96-29.

Eriksen T.E., Eklund U.-B., Werme L.O. and Bruno J., 1995. Dissolution of irradiated fuel: a radiolytic mass balance study. J. Nucl. Mater. 227, 76-82.

Finch R. and Ewing R. (1991). Uraninite alteration in an oxidizing environment and its relevance to the disposal of spent nuclear fuel. SKB Technical Report TR 91-15.

Forsyth R.S. and Eklund U.-B., 1995. Spent nuclear fuel corrosion: The application of ICP-MS to direct actinide analysis. SKB Technical Report TR 95-04.

Forsyth R.S. and Werme L.O., 1992. Spent fuel corrosion and dissolution. J. Nucl. Mater. 190, 3-19.

Forsyth R.S., Werme L.O. and Bruno J, 1986. The corrosion of spent UO_2 fuel in synthetic groundwater. J. Nucl. Mater. 138, 1-15.

Forsgren G., 1988. Development of a method for identification of the oxidation state of uranium oxide surfaces in aqueous media. Examensarbete TITRA-OOK-1022.

Giménez J., Baraj E., Torrero M.E., Casas I. and de Pablo J., 1996. Effect on H_2O_2, $NaClO_4$ and Fe on the dissolution of unirradiated UO_2 in NaCl 5 mol kg^{-1}. Comparison with spent fuel dissolution experiments. J. Nuc. Mater., 238, 64-69.

Grandstaff D.E., 1976. A kinetic study of the dissolution of uraninite. Economic Geology, 8, 1493-1506.

Gray W.J. and Wilson C.N., 1995. Spent fuel dissolution studies FY 1991 to 1994. Pacific Northwest Nat. Lab. Report PNL-10540. UC-802. December 1995.

Gray W.J., Leider H.R. and Steward S.A., 1992. Parametric study of LWR spent fuel dissolution kinetics. J. Nucl. Mater. 190, 46-52.

Grenthe I., Fuger J., Konings R.J.M., Lemire R.J., Muller A.B., Nguyen-Trung C. and Wanner H., 1992. Chemical Thermodynamics Vol.1. Chemical Thermodynamics of Uranium. NEA-OECD. (Wanner and Forest ed.) Elsevier.

Hiskey J.B., 1980. Hydrogen peroxide leaching of uranium in carbonate solutions. Trans. Instn Min. Metall (Sect. C: Mineral Process. Extr. Metall.) 89; C-145,C-152.

Hocking W.H., Betteridge J.S. and Shoesmith D.W., 1994. The cathodic reduction of oxygen on uranium dioxide in dilute alkaline aqueous solution. J. Electroanalytical Chemistry 379, 339-351.

Hocking W.H., Shoesmith D.W. and Betteridge J.S. 1992. Reactivity effects in the oxidative dissolution of UO_2 nuclear fuel. J. Nucl. Mater. 190, 36-45.

Holland, H.D., 1984. The chemical evolution of the atmosphere and the oceans. Princeton Series in Geochemistry (Holland ed.), Princeton, New Jersey, 315-332.

Lasaga A.C., Soler J.M., Ganor J, Burch T.E. and Nagy K.L., 1994. Chemical weathering rate laws and global geochemical cycles. Geochim. et Cosmochim. Acta 58, 2361-2386.

McKibben M.A. and Barnes H.L., 1986. Oxidation of pyrite in low temperature acidic solutions: rate laws and surface textures. Geochim. et Cosmochim. Acta, 50, 1509-1520.

Moses C.O., Nordstrom D.K., Herman J.S. and Mills A.L., 1987. Aqueous pyrite oxidation by dissolved oxygen and by ferric iron. Geochim. et Cosmochim. Acta, 51, 1561-1571.

Nicholson R.V., Gillham R.W. and Reardon E.J., 1988. Pyrite oxidation in carbonate-buffered solution: 1. Experimental kinetics. Geochim. Cosmochim. Acta, 52, 1077-1085.

Ollila K., 1995. Solubility of unirradiated UO_2 fuel in aqueous solutions-Comparison between experimental and calculated (EQ3/6) data. Report YJT-95-14.

Posey-Dowty J., Axtmann E., Crerar D., Borcsik M., Ronk A. and Woods W., 1987. Dissolution rate of uraninite and uranium roll-front ores. Economic Geology, 82, 184-194.

Puigdomènech I. and Bruno J., 1991. Plutonium solubilities. SKB Technical Report TR 91-04.

Shoesmith D.W., Sunder S., Bailey M.G. and Wallace G.J., 1989. The corrosion of nuclear fuel (UO_2) in oxygenated solutions. Corrosion Sci. 29 (9), 1115-1128.

Shoesmith D.W. and Sunder S., 1991. An Electrochemistry-based model lfor the dissolution of UO_2. Atomic Energy of Canada Limited Report AECL - 10488. 97pp.

Shoesmith D.W. and Sunder S., 1992. The prediction of nuclear fuel (UO_2) dissolution rates under waste disposal conditions. J. Nucl. Mater. 190, 20-35.

SKB-91, 1992. Final disposal of spent nuclear fuel. Importance of the bedrock for safety. SKB Technical Report 92-20.

SKI SITE 94, 1996. Deep Repository Performance Assessment Project Vol. I. SKI Report 96:36.

Stumm W. and Furrer G., 1987. The dissolution of oxides and aluminum silicates; Examples of surface-coordination-controlled kinetics in: Aquatic Surface Chemistry. Chemical Processes at the Particle-Water Interface. (W. Stumm ed.) John Wiley and Sons.

Sunder S, Shoesmith D.W., Miller N.H. and Wallace G.J., 1992. Determination of criteria for selecting a UO_2 fuel dissolution model for nuclear fuel waste management concept assessment. Mat. Res. Soc. Symp. Proc. Vol. 257 345-.

Torrero M.E., 1995. Estudio de la disolución del UO_2 como análogo químico de la matriz del combustible nuclear gastado. Influencia de los principales parámetros fisicoquímicos que definen los repositorios en medios salino y granítico. Ph. D. Thesis, Univ. de Barcelona.

Torrero M.E., Baraj E., de Pablo J, Giménez J. and Casas I., 1997. Kinetics of corrosion and dissolution of uranium dioxide as a function of pH. Int. J.Chem. Kinet.29, 261-267.

Williamson M.A. and Rimstidt J.D., 1994. The kinetics and electrochemical rate-determining step of aqueous pyrite oxidation. Geochim. Cosmochim. Acta, 58, 5443-5455.

Wolery T.J., 1992. EQ3NR, A computer program for geochemical aqueous speciation-solubility calculations: Theoretical Manual, User´s Guide, and Related Documentation (Version 7.0). LLNL.

Wronkiewicz D.J., Bates J.K., Gerding T.J., Veleckis E. and Tani B.S., 1992. Uranium release and secondary phase formation during unsaturated testing of UO_2 at 90 ^{o}C. J. Nucl. Mater 190, 101-106.

List of SKB reports

Annual Reports

1977-78
TR 121
KBS Technical Reports 1 – 120
Summaries
Stockholm, May 1979

1979
TR 79-28
The KBS Annual Report 1979
KBS Technical Reports 79-01 – 79-27
Summaries
Stockholm, March 1980

1980
TR 80-26
The KBS Annual Report 1980
KBS Technical Reports 80-01 – 80-25
Summaries
Stockholm, March 1981

1981
TR 81-17
The KBS Annual Report 1981
KBS Technical Reports 81-01 – 81-16
Summaries
Stockholm, April 1982

1982
TR 82-28
The KBS Annual Report 1982
KBS Technical Reports 82-01 – 82-27
Summaries
Stockholm, July 1983

1983
TR 83-77
The KBS Annual Report 1983
KBS Technical Reports 83-01 – 83-76
Summaries
Stockholm, June 1984

1984
TR 85-01
Annual Research and Development Report 1984
Including Summaries of Technical Reports Issued during 1984. (Technical Reports 84-01 – 84-19)
Stockholm, June1985

1985
TR 85-20
Annual Research and Development Report 1985
Including Summaries of Technical Reports Issued during 1985. (Technical Reports 85-01 – 85-19)
Stockholm, May 1986

1986
TR 86-31
SKB Annual Report 1986
Including Summaries of Technical Reports Issued during 1986
Stockholm, May 1987

1987
TR 87-33
SKB Annual Report 1987
Including Summaries of Technical Reports Issued during 1987
Stockholm, May 1988

1988
TR 88-32
SKB Annual Report 1988
Including Summaries of Technical Reports Issued during 1988
Stockholm, May 1989

1989
TR 89-40
SKB Annual Report 1989
Including Summaries of Technical Reports Issued during 1989
Stockholm, May 1990

1990
TR 90-46
SKB Annual Report 1990
Including Summaries of Technical Reports Issued during 1990
Stockholm, May 1991

1991
TR 91-64
SKB Annual Report 1991
Including Summaries of Technical Reports Issued during 1991
Stockholm, April 1992

1992
TR 92-46
SKB Annual Report 1992
Including Summaries of Technical Reports Issued during 1992
Stockholm, May 1993

1993
TR 93-34
SKB Annual Report 1993
Including Summaries of Technical Reports Issued during 1993
Stockholm, May 1994

1994

TR 94-33

SKB Annual Report 1994

Including Summaries of Technical Reports Issued during 1994

Stockholm, May 1995

1995

TR 95-37

SKB Annual Report 1995

Including Summaries of Technical Reports Issued during 1995

Stockholm, May 1996

1996

TR 96-25

SKB Annual Report 1996

Including Summaries of Technical Reports Issued during 1996

Stockholm, May 1997

List of SKB Technical Reports 1998

TR 98-01

Global thermo-mechanical effects from a KBS-3 type repository. Summary report

Eva Hakami, Stig-Olof Olofsson, Hossein Hakami, Jan Israelsson

Itasca Geomekanik AB, Stockholm, Sweden

April 1998

TR 98-02

Parameters of importance to determine during geoscientific site investigation

Johan Andersson[1], Karl-Erik Almén[2], Lars O Ericsson[3], Anders Fredriksson[4], Fred Karlsson[3], Roy Stanfors[5], Anders Ström[3]

[1] QuantiSci AB

[2] KEA GEO-Konsult AB

[3] SKB

[4] ADG Grundteknik KB

[5] Roy Stanfors Consulting AB

June 1998

TR 98-03

Summary of hydrochemical conditions at Aberg, Beberg and Ceberg

Marcus Laaksoharju, Iona Gurban, Christina Skårman

Intera KB

May 1998

TR 98-04

Maqarin Natural Analogue Study: Phase III

J A T Smellie (ed.)

Conterra AB

September 1998

TR 98-05

The Very Deep Hole Concept – Geoscientific appraisal of conditions at great depth

C Juhlin[1], T Wallroth[2], J Smellie[3], T Eliasson[4], C Ljunggren[5], B Leijon[3], J Beswick[6]

[1] Christopher Juhlin Consulting

[2] Bergab Consulting Geologists

[3] Conterra AB

[4] Geological Survey of Sweden

[5] Vattenfall Hydropower AB

[6] EDECO Petroleum Services Ltd.

June 1998

TR 98-06

Indications of uranium transport around the reactor zone at Bagombe (Oklo)

I Gurban[1], M Laaksoharju[1], E Ledoux[2], B Made[2], A L Salignac[2],

[1] Intera KB, Stockholm, Sweden

[2] Ecole des Mines, Paris, France

August 1998

TR 98-07

PLAN 98 – Costs for management of the radioactive waste from nuclear power production

Swedish Nuclear Fuel and Waste Management Co

June 1998

TR 98-08

Design premises for canister for spent nuclear fuel

Lars Werme

Svensk Kärnbränslehantering AB

September 1998

TR 98-09

Test manufacturing of copper canisters with cast inserts Assessment report

Claes-Göran Andersson

Svensk Kärnbränslehantering AB

Augusti 1998

TR 98-10
Characterization and Evaluation of Sites for Deep Geological Disposal of Radioactive Waste in Fractured Rocks
Proceedings from The 3rd Äspö International Seminar, Oskarshamn, June 10–12, 1998-11-10
Svensk Kärnbränslehantering AB
September 1998

TR 98-11
Leaching of 90-year old concrete mortar in contact with stagnant water
Jan Trägårdh, Björn Lagerblad
Swedish Cement and Concrete Research Institute
July 1998

TR 98-12
Geological-structural models used in SR 97
Uncertainty analysis
Pauli Saksa, Jorma Nummela
FINTACT Ltd
October 1998

TR 98-13
Late Quaternary changes in climate
Karin Holmgren and Wibjörn Karlén
Department of Physical Geography
Stockholm University
December 1998

TR 98-14
Partitioning and transmutation (P&T) 1997
Åsa Enarsson, Anders Landgren, Jan-Olov Liljenzin, Mats Skålberg, Lena Spjuth
Department of Nuclear Chemistry, Chalmers University of Technology, Gothenburg
and
Waclaw Gudowski, Jan Wallenius
Department of Nuclear and Reactor Physics, Royal Institute of Technology, Stockholm
May 1998

TR 98-15
Studies of surface complexation of H^+, NpO_2^+, Co^{2+}, Th^{4+} onto TiO_2 and H^+, UO_2^{2+} onto alumina
Anna-Maria Jakobsson, Yngve Albinsson
Department of Nuclear Chemistry, Chalmers University of Technology, Sweden
and
Robert S Rundberg
Los Alamos National Laboratory, USA
November 1998

TR 98-16
Backfilling with mixtures of bentonite/ ballast materials or natural smectitic clay?
Roland Pusch
Geodevelopment AB
October 1998

TR 98-17
Groundwater degassing in fractured rock:
Modelling and data comparison
Jerker Jarsjö and Georgia Destouni
Water Resources Engineering
Royal Institute of Technology, Stockholm
November 1998

TR 98-18
The interaction of sorbing and non-sorbing tracers with different Äspö rock types
Sorption and diffusion experiments in the laboratory scale
Johan Byegård, Henrik Johansson, Mats Skålberg
Department of Nuclear Chemistry, Chalmers University of Technology, Gothenburg, Sweden
and
Eva-Lena Tullborg
Terralogica AB, Gråbo, Sweden
November 1998

TR 98-19
Äspö Hard Rock Laboratory
Annual Report 1997
Svensk Kärnbränslehantering AB
May 1998

TR 98-20
The biosphere at Aberg, Beberg and Ceberg
– a description based on literature concerning climate, physical geography, ecology, land use and environment
Tobias Lindborg, Regina Schüldt
NaturRådet
December 1998

TR 98-21
Crustal structure and regional tectonics of SE Sweden and the Baltic Sea
Alan Geoffrey Milnes
Department of Geology, University of Bergen, Norway
David G Gee and Carl-Erik Lund
Department of Earth Sciences, Uppsala University
November 1998